MACTEC

March 26, 2004

40-8907

3410030048.07

Mark D. Purcell
Remedial Project Manager
Superfund Division
United States Environmental Protection Agency
Region 6
1445 Ross Avenue, Suite 1200
Dallas, TX 75202-2733

Hydraulic Fracturing of Zone 3
United Nuclear Corporation Church Rock Superfund Site
Administrative Order (Docket No. CERCLA 6-11-89)

Dear Mr. Purcell:

On behalf United Nuclear Corporation (UNC), MACTEC Engineering and Consulting (MACTEC) has prepared this letter to respond to comments presented by the United State Environmental Protection Agency (USEPA) and the Navajo Nation Environmental Protection Agency (Navajo Nation EPA) on our December 23, 2003 report entitled "Final Report, Hydraulic Fracturing Pilot Test Results and Preliminary Full Scale Design, United Nuclear Church Rock Facility". USEPA comments, which also provided comments from the New Mexico Environment Department (NMED) were provided in a letter dated March 10, 2004. Comments from the Navajo Nation EPA were provided in a letter dated March 11, 2004.

USEPA COMMENTS

The US EPA letter provided two General Comments and two Specific Comments. We have provided each comment below in italics with our associated response.

USEPA General Comment 1

The United States Environmental Protection Agency (EPA) and the New Mexico Environment Department (NMED) are concerned that fractures induced by the hydraulic fracturing of Zone 3 may propagate in unwanted directions, causing the spread of contamination or naturally occurring petroleum deposits (oil) in the area. For example, fractures that propagate downward through the shale and lignite of Zone 2 and into the underlying Zone 1, causing the downward migration of contamination from Zone 3 into Zone 1.

In light of such concerns, please modify the Report on Hydraulic Fracturing Pilot Test Results and Preliminary Full Scale Design (Report) to include a contingency plan for stopping the hydraulic fracturing operation in the event that induced fractures propagate in the underlying Zone 1 or an oil bearing zone. Also specify in the contingency plan how the induced fractures shall be sealed in the even that they penetrate into such Zones. Further, describe how the operator will know if, and when, the propagating fractures penetrate into Zone 1 or and oil-bearing zone. Finally, specify as a contingency that additional monitoring wells will be constructed into Zone 1 to monitor water

MACTEC Engineering and Consulting
Carnegie Office Park, Bldg. 4, 700 N. Bell Avenue, Suite 200 • Pittsburgh, PA 15106
412-279-6661 • Fax: 412-279-8567

NMSS01

chemistry in the area of the propagating fractures should they propagate downward into Zone 1. Specify that the number and location of Zone 1 monitoring wells shall be determined based on the results of the hydraulic fracturing operation and subsequent approval by the EPA. Also specify that the frequency and duration of the Zone 1 groundwater monitoring, if performed, shall be determined by EPA.

UNC and MACTEC appreciate and share your concerns. As you know, hydraulic fracturing has been performed in oil and gas operations since the early 1950's. However, fracturing rock at approximate depths of 200 feet or less as we propose is not a routine application of the technology. Although UNC and MACTEC believe that fracturing operations will not adversely impact the existing plume, there is no way to guarantee how the rock will fracture. This concern was one of the reasons that the pilot test was conducted in the un-impacted portion of Zone 3.

Results from the pilot test indicate that the induced fracture in the open boring stage (Stage 1) extended horizontally, with no vertical component. The induced fracture in the cased and perforated stage (Stage 2) began to propagate horizontally, then instantaneously "jumped" to a shallower depth before continuing to propagate horizontally. Our fracture diagnostics contractor, Pinnacle Technologies, believes that it is likely that the fracture "jump" observed in the second stage of the pilot test was caused when the induced fracture intersected the observation well that was cemented prior to the pilot test. It is Pinnacle's belief that the observation well may not have been adequately sealed before the pilot test and when the induced fracture encountered the well, the fracture propagated up a weakness or channel in the cement to an unconsolidated formation at a shallower depth, and then continued horizontally through that zone. The higher observed treating pressures associated with Stage 2 (likely required to overcome friction loss from pumping the treatment through the perforations) may have contributed to the "jump". Based on these pilot test results, MACTEC recommended that future fracturing be done using the "open boring" approach and that all nearby existing wells be sealed with a high quality cement job prior to fracturing.

MACTEC and UNC are in agreement that a contingency plan is needed. A contingency plan that covers the issues highlighted in your comment is included as Attachment A to this letter. The contingency plan will include "real time" monitoring of fracturing operations by Pinnacle that will allow prompt shut down of pumping operations if a vertical component or "jump" is detected. During fracturing operations, water is used to initiate the fracture and proppant (sand) is not started until treating pressures stabilize. Therefore, the leading edge of the induced fracture would likely have fluid (water) without sand. If a vertical component or "jump" is noted by Pinnacle and fracturing operations are ceased (fluid pressure is relaxed), the portion of the fracture that deviated from horizontal would not likely have proppant. As soon as the fluid pressure is relaxed, the fracture closes back with little if any increase in conductivity along the fracture, unless propped open by sand[1]. Therefore it is unlikely that a significant undesired preferential pathway would remain. In the event of an undesired excursion of induced fractures into Zone 1, USEPA reserves the authority to require monitoring wells in Zone 1 in whatever number and for whatever duration as appropriate.

USEPA General Comment 2

Please include with the revised Report, supporting documentation such as case studies to substantiate UNC's/MACTEC's claim about the rock mechanics and anticipated fracture direction for Zone 3

[1] Allen, Thomas O. and Roberts, Alan P., 1982. Production Operations, v. 2, p.114.

which was discussed at the February 26, 2004 meeting with EPA and other regulatory agencies (i.e., hydraulic fracturing will most likely cause induced fractures to propagate upward within Zone 3, rather than downward through the underlying shale and coal layers of Zone2 and into Zone 1).

Attachment B contains a document published by the U.S. Geological Survey that describes the mechanics involved with induced fracture propagation in shallow hydraulic fracturing. Normally, fractures will be propagated in a direction perpendicular to the least principal stress. At shallow depths, the vertical stress (overburden stress) is usually less than the horizontal stresses, therefore the fracture propagates horizontally.

USEPA Specific Comment 1: Section 4.2 – Recovery Well Installation, page 4-4, Item 3

Provide details of the chemical composition of Super CBL® or Microbond® in an appendix and include an evaluation of such material to ensure that they will not introduce harmful substances into the ground water. These materials are proposed to be used as bonding agents in the cement used to fill the well annular space.

Attachment C contains Material Safety Data Sheets (MSDSs) for both additives. Both additives are insoluble in water. Super CBL® and Microbond® have been used in tens of thousands of oil and gas wells as an additive in cement to improve bonding. To our knowledge, there have been no reports of adverse impacts to groundwater from the use of these materials

USEPA Specific Comment 2: Section 4.2 – Recovery Well Installation, page 4-5, Item 5

The paragraph states that pea gravel and sand will be placed at the bottom of the well to reduce the chance of the induced fracture propagating down the well and into the coal. Please provide documentation that supports such design.

Small diameter (AX-Diameter) core drilling will be conducted to determine the actual depth to the base of Z-3 at the location of each recovery well. To minimize the depth of over drilling the base of Z-3, core runs of two feet will be drilled. Upon determination of the depth of the base of Zone 3 by coring, pea gravel will be placed into the well to fill the core hole to a level above the base of Z-3. It is anticipated that less than two feet of pea gravel would be placed to accomplish this. The well will then be reamed to a final depth approximately 0.5 to 1 foot above the base of Z-3. The diameter of the open hole will be as large as practical, given the 7-inch diameter casing above the open hole. A mixture of pea gravel and medium sand will be placed at the bottom of the well to fill the remaining small diameter portion of the boring. This layer will be topped with approximately 0.2 feet of fine sand.

The effectiveness of placing pea gravel and sand to reduce the potential for the fracture to propagate down the well and into the coal is based on field experience. A common technique used to complete a multiple stage fracture treatment in a shallow oil well is to fill the well with pea gravel, set a single element packer on frac pipe just above the zone to be fractured, complete the fracture treatment, wash down through the pea gravel (flushing out some of the pea gravel to the next zone of interest, which is frequently only a few feet lower than the first zone), set the packer again and fracture the second zone. This procedure is repeated so that multiple zones are fractured. When hydraulic pressure is applied during fracturing operations, the pea gravel apparently "screens off" and impedes fracturing fluid migration downward through the rest of the boring. This causes the pressure to build quicker in the open boring than in the portion of the boring filled with the sand and pea gravel mixture. Therefore, the fracture initiation pressure is first reached in the open boring. Once the fracture is initiated at the desired interval, hydraulic pressure in the boring drops and fracturing fluid travels in the path of least resistance, which is through the induced fracture.

NAVAJO NATION EPA COMMENTS

The Navajo Nation EPA letter provided eight comments and five additional comments from the Navajo Nation EPA's Underground Injection Control Program. We have provided each comment below with our associated response.

(1) There are numerous borings that exist throughout the area of the Zone 3 plume. From the data associated with these borings, is UNC able to sufficiently characterize the subsurface structural geology in terms of identifying fractures, voids, and other potential conduits? These numerous borings within the area of the Zone 3 plume are potential points for short-circuiting.

We agree that the presence of numerous borings that penetrate Zone 3 at the site is an important consideration. The rationale for selecting the locations of the proposed recovery wells was, in part, dictated by the presence of old borings. Because pilot test results indicate that an induced fracture with a radius of approximately 34-45 feet was propagated during Stage 1, we believe that we have mitigated the potential for short circuiting by locating proposed recovery wells in areas that have a minimal number of existing wells within 100 feet. Only one well (PB-01) appears to be within 100 feet of proposed recovery wells and will be plugged prior to hydraulic fracturing operations. Data from the pilot test indicate that there are few, if any, naturally occurring fractures at the base of Zone 3 in the area of the pilot test; however, we realize fractures may be present in other areas and that is one reason we have located recovery wells in areas that are, for the most part, at least 100 feet away from existing borings.

(2) What are the in-situ stresses expected in Zone 3 and in the surrounding layers? Hydraulic fracturing will propagate perpendicular to the minimum principal stress in a formation. What is the fluid efficiency expected for the proposed hydraulic fracturing?

We anticipate the vertical stress at this shallow depth to be less than the horizontal stresses; therefore the fractures are expected to propagate horizontally. Fracture gradients noted during the pilot test were greater than 1, indicating the propagation of a horizontal fracture. Based on the pilot test, Halliburton calculated fluid efficiency to be approximately 8% to 10%. This means that by the end of the job, approximately 90% of the fresh water had leaked-off into the sandstone matrix.

(3) During hydraulic fracturing of Zone 3, if the propagated fracture vertically migrates to the surface the hydraulic fracturing will cease and the fracture will be allowed to close in on itself. UNC has proposed seven recovery wells (RW-11 to RW-17). If there is any excursion encountered during hydraulic fracturing, how will this impact the placement of the recovery wells. How much displacement will be needed to relocate a hydraulic fracturing/recovery well locale?

Both Halliburton data and Pinnacle data will be evaluated if an excursion is encountered. Depending on the data, corrective actions that may be considered include, but are not limited to, adjustment of pumping rates, reduction of total fluid amounts, and other changes to the treatment design. At this time, it is not anticipated that recovery wells will be relocated.

(4) The fracture conductivity is the sum of the propped fracture width and the permeability of the propping agent. This conductivity will reduce with time due to increasing stress on the fracture, stress corrosion affecting proppant strength, proppant crushing, and proppant embedment into the formation. Will the proposed recovery wells be affected by this type of reduction of fracture conductivity? What is the expected life of these proposed recovery wells?

While it is likely that induced fracture conductivity will decrease with time, at these shallow depths we do not believe that proppant strength or proppant crushing will be an issue (there may be some embedment). The expected life of the proposed recovery wells is approximately ten years and we believe that the fracture conductivity during that timeframe will be sufficient to accomplish the goals of the project.

(5) UNC proposes to use sand as a propping agent in the hydraulic fracturing. If results of the fracturing are not favorable will UNC opt to use another propping agent?

We do not plan to use ceramic proppants or any other propping agents at this time.

(6) Fracture diagnostics for the proposed hydraulic fracturing will involve the use of surface tilt meters in a 32-unit array (for each well?). During Stage 2 of the pilot hydraulic fracturing operations, where the induced fracture moved up vertically 50 feet, the tilt meter array used did not detect a vertical component at the time. Will use of surface tilt meters be sufficient to detect any and all undesired vertical prolongations? Downhole tilt meters at depths near the zone to be fractured are useful for determining fracture height.

Pinnacle Technologies proposes to have two 60 tool arrays that will cover the two recovery well areas (the RW-11 to RW-14 area and the RW-15 to RW-17 area). Pinnacle determined that there was not a vertical component, but rather an instantaneous "jump" of the fracture. They believe that this "jump" was cause by short circuiting through the first pilot test boring due.

As discussed at our meeting, with respect to downhole tilt meters, we agree and plan to use them (see attached contingency plan).

(7) The Zone 3 plume is migrating in a north-northeast direction. Increases in alkalinity in the ground water are the precursors to increases in pH and metals. The northern-most monitoring well (NBL-01), prior to reaching the Navajo Nation boundary, is reportedly showing an increase in alkalinity. The proposed hydraulic fracturing is intended to stop the plume from advancing further northward. Is there a need to install another monitoring well further north of NBL-01 in Section 36 to assess whether the plume has stopped advancing? What are the conditions of the existing monitoring wells located near the Navajo Nation boundary?

Increasing alkalinity is not a precursor to increasing pH and metals concentrations. Increasing alkalinity is an indication that seepage-impacted water is beginning to dissolve carbonate rock in the formation. After some years (usually 3 to 4), when the available carbonate buffering is used up, the alkalinity will drop, eventually reaching zero. It is after this that the pH drops and metals concentrations rise. Well NBL-01 has not shown this pattern; and is therefore considered an un-impacted well. There is no reason to install an additional well at this time. The existing wells are in good condition.

(8) How will U.S. EPA measure success of the hydraulic fracturing? At what point (i.e., decrease in well pumping rates) will U.S. EPA decide that the hydraulic fracturing is not successful?

USEPA will provide a response to this comment.

The following comments were supplied by staff from Navajo EPA's Underground Injection Control Program:

(1) Naturally occurring fractures at the facility site could act as conduits to the surface upon fracture stimulation.

We agree that this is possible but, as previously discussed, have taken steps to reduce the potential for migration of the fracture to the surface. We will also take steps as outlined in the attached contingency plan to reduce the potential for induced fractures to cause migration problem if the fracture deviates from horizontal.

(2) Since the zone in question (Gallup Sandstone Formation) crops out at the site, there is no overlying confining rock layer to contain the frac.

No overlying confining rock layer is needed since the anticipated and desired orientation of the induced fracture is horizontal. Overlying confining rock layers are usually an issue in deeper fracturing programs where a vertical fracture is predicated (and usually desired to interconnect multiple "pay" horizons).

(3) Typically, the fracture gradient of a zone is estimated at 0.2 psi/ft of depth. At the very shallow depth of 200', the calculated fracture point of the rock is only 40 psi; the fracture pressures in MACTEC's report (225-2982 psi.) far exceed this maximum pressure value.

Halliburton data from the pilot test (Appendix C of our Report) indicate that the observed fracture gradient was 1.18 psi/ft in Stage 1 and 1.25 psi/ft in Stage 2. Based on discussion with Halliburton, a fracture gradient of 0.2 psi/ft would be anomalously low for this region.

(4) The recommended open-hole frac may be more difficult to control than a cased-hole frac, i.e., the frac may not go horizontally as designed.

Pilot test results indicate that open hole fracturing (Stage 1 of the pilot test) produced better results than cased hole fracturing (Stage 2). MACTEC, Halliburton, and Pinnacle do not believe that inducing and maintaining a horizontal fracture will be more difficult in an open hole.

(5) Typically, "frac jobs" have "sled runner" configurations, i.e., the induced fractures begin horizontally, but eventually turn vertically at their terminus. At the very shallow depths at this site, this means that the fractures could break to surface.

Halliburton, Pinnacle, and MACTEC are not aware of "sled runner" configurations in typical frac jobs.

Should you have any questions regarding the above responses to your comments, please do not hesitate to contact Pat Pontoriero at (412) 279-6661. We look forward to continuing our work with you on this project.

Respectfully submitted,

MACTEC Engineering and Consulting

Pat Pontoriero, P.G.
Senior Principal Geologist

Dayne M. Crowley, P.G.
Senior Principal Hydrogeologist

PP\DMC: na

cc: Roy Blickwedel, GE Corporate Environmental Programs
Larry Bush, United Nuclear Corporation
William von Till, Nuclear Regulatory Commission
Robin Brown, New Mexico Environment Department
Diana Malone, Navajo Nation EPA

P:/PROJECTS/GE CORPORATE/3410030048 Church Rock, NM/FINAL/EPA Response Letter.doc

ATTACHMENT A

CONTINGENCY PLAN

CONTINGENCY PLAN
PRELIMINARY FULL SCALE DESIGN
UNITED NUCLEUR CHURCH ROCK FACILITY

Purpose

The purpose of this contingency plan is to outline a mechanism for quickly stopping hydraulic fracturing operation in the event that induced fractures propagate in the underlying Zone 1 or into an overlying oil bearing zone. This contingency plan describes how "real time" monitoring of fracturing operations will be completed by Pinnacle Technologies (Pinnacle) to allow prompt shut down of pumping operations if a vertical component or "jump" is detected.

Background

During fracturing operations, water is used to initiate the fracture and proppant (sand) is not started until treating pressures stabilize. Therefore, the leading edge of the induced fracture would likely have fluid (water) without sand. If a vertical component or "jump" is noted by Pinnacle and fracturing operations are promptly ceased (fluid pressure is relaxed), the portion of the fracture that deviated from horizontal would not likely have proppant. As soon as the fluid pressure is relaxed, the fracture closes back with little if any increase in conductivity along the fracture, unless propped open by sand[2]. Therefore it is unlikely that a significant undesired preferential pathway would remain.

The goal of the fracture monitoring program is to provide direct measurements of horizontal fracture growth from vertical recovery wells at the Site. To minimize the number of vertical drain holes yet maximize drainage efficiency, it is imperative to know 1) the orientation of the created hydraulic fracture(s) and 2) the aerial extent or growth of such hydraulic fractures. The orientation is critical to achieve adequate inflow to the vertical drain holes and the aerial extent of the hydraulic fractures will determine the required density of drain holes.

In 2003, a test Recovery Well (the HF-3) was drilled and hydraulically fractured outside the area of proposed remediation. To monitor the growth and coverage of the created hydraulic fracture, an array of 32 surface tiltmeters was installed covering a surface area surrounding the HF-3 well extending out from the wellbore approximately 250% the depth of the hydraulic fracture. For example, a drain hole having a hydraulic fracture initiated at a depth of 160 ft from the surface would have a surface tiltmeter array surrounding the wellhead approximately 400+ ft in all directions. The 2003 test project was designed (from a surface tiltmeter mapping perspective) to determine the 1) the vertical component (if any) created from the hydraulic fracturing operations, 2) the radial extent of the created horizontal fracture(s), and 3) would the surface deformation caused by the hydraulic fracturing affect a nearby LPG pipeline.

The answers found to the above questions in 2003 were 1) No vertical growth was observed, 2) the radial extent of the hydraulic fracture was between 35 and 45 ft in radius, and 3) surface ground movements of <0.1 inch was within pipeline design limits.

---

[2] Allen, Thomas O. and Roberts, Alan P., 1982. Production Operations, v. 2, p.114.

Fracture Monitoring Program

Based on Pilot Test results and the anticipated location of recovery wells for the first phase of full scale implementation, two separate surface tiltmeter arrays of approximately 60 sites each will be required to image all seven recovery wells. Well R11, R12, R13, & R14 will be covered with one array and wells R31, R32, & R33 will be imaged with the second array. Some of the surface tiltmeter sites from the 2003 project will be reused for the 2004 mapping project.

To provide real time monitoring of hydraulic fracturing operations, hydraulic fracture treatments in seven Recovery Wells will be mapped utilizing both surface and real-time downhole tiltmeter mapping services. To map hydraulic fracture growth in real-time, an array of 10 downhole tiltmeter tools will be placed in multiple vertical wellbores offsetting the recovery wells (see Figure 1). The lateral distance between the recovery well being treated and the vertical observation well will be at least 100 ft but not more than 500 ft away. The closer the observation well to the treatment well(s), the better the fracture height (vertical movement) measurement resolution. We estimate the vertical resolution at 500 ft away from the treatment well to be within 5 ft. This should provide adequate vertical resolution for compliance with project requirements.

To obtain the best possible hydraulic fracture growth images, the downhole tiltmeter array will essentially straddle the intended fracture interval. A diagram of this is shown in Figure 2. It may be necessary to drill specific observation wells for this purpose.

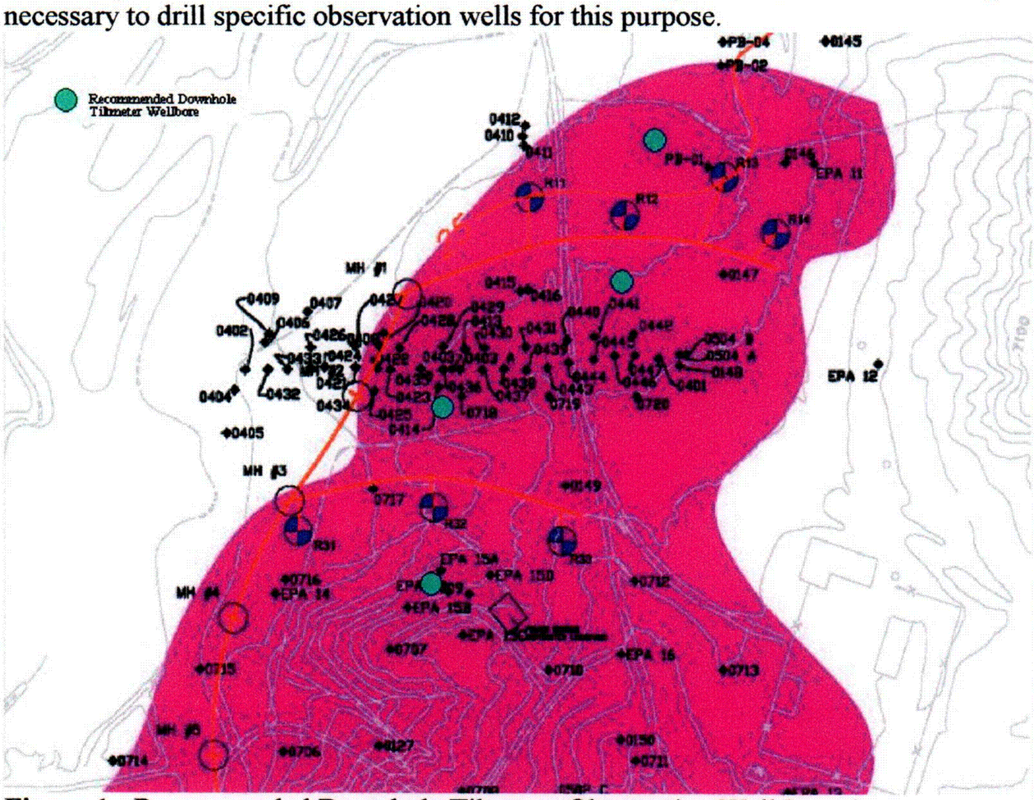

Figure 1: Recommended Downhole Tiltmeter Observation Well Locations

The surface array will identify aerial extent, vertical, and horizontal components of the hydraulic fracture(s). The downhole tiltmeters will provide real-time measurement of the created hydraulic fracture height and vertical (if any) movement.

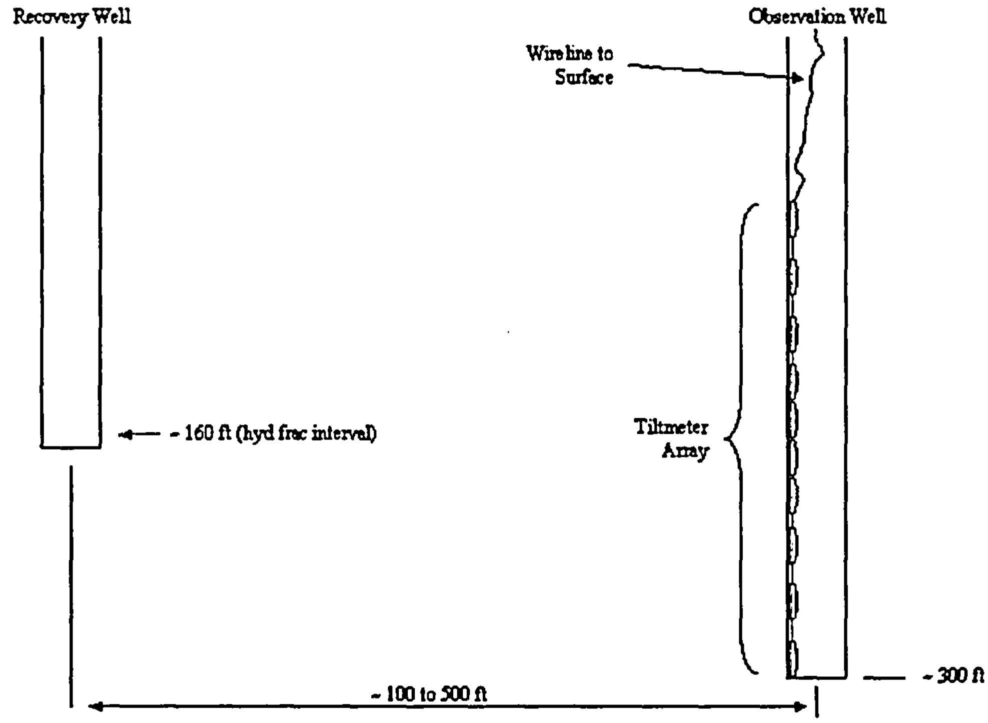

Figure 2: Generic Schematic for Downhole Tiltmeter Installation

Contingency Plan

To allow the hydraulic fracturing operator to know if, and when, the propagating fractures penetrate into Zone 1 or and oil-bearing zone, a Pinnacle Technician will monitor fracturing operations in the Halliburton operations truck. If data indicate that the fracture is propagating into Zone 1 or and upper, oil bearing zone, fracturing operations will be promptly shut down.

Should induced fractures propagate downward into Zone 1 and at USEPA's request, additional monitoring wells could be constructed into Zone 1 to monitor water chemistry in the area of the propagating fractures. The number and location of Zone 1 monitoring wells, as well as the frequency and duration of monitoring, would be determined based on the results of the hydraulic fracturing operations and subsequent approval by the EPA.

ATTACHMENT B

USGS PAPER

the surface of an elastic earth. Ge
9, 29–35, 1944.

(Received May 6, 1969.)

JOURNAL OF GEOPHYSICAL RESEARCH VOL. 74, NO. 25, NOVEMBER 15, 1969

Theoretical Size of Hydraulically Induced Horizontal Fractures and Corresponding Surface Uplift in an Idealized Medium

REN JEN SUN

U. S. Geological Survey, Washington, D. C. 20242

For the disposal of radioactive wastes by hydraulic fracturing and grout injection, it is considered essential that the induced fractures be nearly horizontal. Bottom-hole injection pressure in excess of overburden pressure has been recognized as one indication that fracturing is horizontal. The amount of uplift of the ground surface caused by the injection can be used as another indicator. For an impervious, homogeneous, isotropic medium, a mathematical model for calculating the amount of uplift of the ground surface, the maximum separation of the horizontally induced fracture at the injection well site, and the radius of extension of the fracture was developed from the basic formulas derived by I. N. Sneddon (1946) and A. E. Green (1949). If the bottom-hole injection pressure is greater than the overburden pressure, and the observed uplift is nearly the same as the calculated uplift, the fracture orientation probably is nearly horizontal. Uplift from nine injections made at the Oak Ridge National Laboratory, Tennessee, from 1960 through 1965, have been used to test the validity of the mathematical model. The calculations agree reasonably well with the observed data.

INTRODUCTION

Since hydraulic fracturing was introduced to the petroleum industry in 1948 [*Clark*, 1949], the technique has been improved greatly, particularly in the last decade. In 1958 the Oak Ridge National Laboratory (ORNL), Tennessee, began to study the feasibility of radioactive waste disposal into a shale formation by hydraulic fracturing. The requirements for this type of waste disposal are as follows: (1) the fracture should be horizontal or nearly horizontal; (2) the waste should be trapped in a certain known area; and (3) there should be no leakage through the enclosing formation which might contaminate aquifers above or below the fractured zone.

The existing theories indicate that the orientation plane of hydraulic fractures is normal to the least compressive stress [*Hubbert*, 1951; *Odé*, 1956; *Hubbert and Willis*, 1957; *Cleary*, 1958*a*, *b*; *Lamont and Jessen*, 1963]. The direction of the least compressive stress can be vertical, horizontal, or inclined, depending on the regional tectonic conditions and on the strength of the rock. The rock strength is especially significant when the hydraulic fracturing is done at shallow depths. A horizontal fracture can be formed only in an area where the least compressive stress is in the vertical direction and is simply equal to the overburden pressure caused by the weight of the overlying rocks.

The orientation of the fracture produced, either horizontal or vertical, is suggested by the hydraulic injection pressure, which is defined as the hydraulic pressure necessary for parting the formation continuously during the injection. If the injection pressure is greater than the overburden pressure of the formation, then the fracture formed may be horizontal; otherwise, it must be vertical or nearly so. It has been observed that usually the injection pressure for forming a vertical fracture is about three-quarters of the overburden pressure [*Harrison et al.*, 1955; *Hubbert and Willis*, 1957; *Crittendon*, 1959; *Fraser and Pettitt*, 1962].

If the direction of the least compressive stress is known, the orientation of a hydraulically induced fracture can easily be predicted. Unfortunately, the magnitude and direction of the regional tectonic stresses are hard to determine. By carefully studying the regional geological structures, such as faults and folds or other evidence, it may be possible to determine the

Copyright © 1969 by the American Geophysical Union.

tectonic stresses that existed when the faults or folds were formed. However, the existing stresses may be entirely different at the present time. Thus, geological structures can be used only as guides in studying the feasibility of forming a horizontal fracture.

Since it is not known beforehand whether a horizontal or nearly horizontal fracture will be formed, it is necessary to test the formation by hydraulic fracturing with water or grout before any actual waste disposal is attempted. The hydraulic injection pressure may suggest the attitude of the fracture formed. However, this information alone cannot be considered sufficient when disposal of radioactive waste is involved. Further information about the orientation of the fracture formed can be obtained by injecting a grout into the formation, allowing it to harden, and then drilling a series of core holes to determine the location and orientation of the grout sheet. Since this procedure is costly, other techniques are desirable.

From 1960 through 1965, ORNL adapted and developed hydraulic fracturing methods of disposal of waste into a dense shale formation. Study of cores made after grout injections showed that the fractures were concordant with the nearly horizontal bedding. The fact that the hydraulic injection pressure at the Oak Ridge site was, in all cases, greater than the formation overburden pressure, shows that under the stress conditions at the site, injection pressure was a valid indicator of possible horizontal fracturing. It was also found that the ground surface around the injection wells had been uplifted during the injections and that the amount of uplift appeared to be related to the injected volume [*DeLaguna*, 1966; *McClain et al.*, 1966].

If a theoretical relation between the injection pressure, injection volume, and amount of uplift can be found, the observed uplift could be another valuable indicator of the horizontal orientation of an induced fracture. If the fracture is horizontal, the observed and theoretical uplift should be nearly the same. The actual uplift can be precisely and readily measured on the ground surface. The purpose of this paper is to develop a theoretical model to calculate the amount of uplift produced by hydraulic fracturing.

Nomenclature

- a, Radius of hydraulically induced fracture.
- a', Maximum radius of the stress-altered region.
- B, Maximum separation of hydraulically induced fracture.
- D, Inside diameter of pipe.
- E, Young's modulus.
- f, Fanning frictional factor.
- h, Depth of the hydraulically induced fracture below the ground surface.
- K', Fluid consistency index, kg = sec$^{N'}$/cm^2.
- N', Fluid-flow behavior index, dimensionless.
- L, Length of pipe.
- Re, Reynold's number.
- p, Pressure in the hydraulically induced fracture.
- p_0, Injection pressure at the injection well site.
- p_h, Static pressure of water in the well.
- Δp, Frictional pressure drop.
- Q, Total injection volume.
- R_1, R_2, Complex distance.
- r, θ, z, Cylindrical coordinates.
- U, V, W, Components of displacement in the radial, tangential, and vertical directions, respectively.
- v, Fluid velocity.
- x, y, z, Cartesian coordinates.
- x', y', z, Cartesian coordinates.
- σ, Normal stress.
- τ, Shear stress.
- λ, μ, Lamé constants.
- Φ_1, Φ_2, Φ_3, Stress functions.
- γ, Average specific weight of rock plus the contained water.
- α, a/a'.
- ρ, Fluid density.
- η, Viscosity.
- ν, Poisson ratio.

General Solutions for an Elastic Body

The problem in the calculation of uplift is to analyze the deformation of a mass of rock resulting from the injection of a known volume of fluid through a well and out into an induced horizontal fracture. For this analysis, the rock considered to be isotropic and homogeneous and to have a linear stress-strain relationship. The infiltration of the injected fluid into the rock adjacent to the induced fracture is assumed to be so small that it can be neglected in the mathematical model; that is, the rock is essentially impermeable. It is also assumed that the injected fluid flows out radially from the injection well into a circular disk-shaped fracture formed by the hydraulic pressure.

Because of the symmetry of the fracture, the cylindrical coordinates r, θ, and z are employed. The polar coordinates r and θ define the position of an element in the x-y plane of a cross section. Thus, $r^2 = x^2 + y^2$. The normal components of stress (σ) and shear stress (τ), and the displacement in the radial, tangential and vertical directions respectively are denoted as σ_r, σ_θ, σ_z; τ_{rz}, $\tau_{r\theta}$, $\tau_{z\theta}$; and U, V, W. By symmetry, V, $\tau_{z\theta}$, and $\tau_{r\theta}$ are zero.

To solve the problem of calculating uplift from hydraulically induced fractures, it is necessary to consider not only the conditions of equilibrium and the distribution of stresses and displacements, but also the boundary conditions of the region in which the solution of the equilibrium equations is developed.

The general equations of equilibrium for an isotropic elastic body in the absence of body force are [*Love*, 1934, p. 143; *Dean et al.*, 1944; *Timoshenko and Goodier*, 1951, p. 343]

$$\begin{aligned} \frac{\partial \sigma_r}{\partial r} + \frac{\partial \tau_{rz}}{\partial z} + \frac{\sigma_r - \sigma_\theta}{r} &= 0 \\ \frac{\partial \tau_{rz}}{\partial r} + \frac{\partial \sigma_z}{\partial z} + \frac{\tau_{rz}}{r} &= 0 \end{aligned} \qquad (1)$$

The displacement and components of stress found by *Dean et al.* [1944] are

$$U = -\frac{1}{2}\frac{\partial \Phi}{\partial r} - \frac{(\lambda + \mu)}{2\mu} z \frac{\partial^2 \Phi}{\partial r\, \partial z} \qquad (2a)$$

$$W = \frac{(\lambda + 2\mu)}{2\mu}\frac{\partial \Phi}{\partial z} - \frac{(\lambda + \mu)}{2\mu} z \frac{\partial^2 \Phi}{\partial z^2} \qquad (2b)$$

$$\sigma_r = \lambda \frac{\partial^2 \Phi}{\partial z^2} - \mu \frac{\partial^2 \Phi}{\partial r^2} - (\lambda + \mu) z \frac{\partial^3 \Phi}{\partial r^2\, \partial z} \qquad (3a)$$

$$\sigma_z = (\lambda + \mu)\left(\frac{\partial^2 \Phi}{\partial z^2} - z\frac{\partial^3 \Phi}{\partial z^3}\right) \qquad (3b)$$

$$\sigma_\theta = \lambda \frac{\partial^2 \Phi}{\partial z^2} - \frac{\mu}{r}\frac{\partial \Phi}{\partial r} - \frac{(\lambda + \mu)}{r} z \frac{\partial^2 \Phi}{\partial r\, \partial z} \qquad (3c)$$

$$\tau_{rz} = -(\lambda + \mu) z \frac{\partial^3 \Phi}{\partial r\, \partial z^2} \qquad (3d)$$

where Φ is a harmonic stress function, that is $\nabla^4\Phi = 0$. In these equations λ and μ are the Lamé constants, which can be expressed in terms of Young's modulus E and the Poisson ratio ν and are given by the expression

$$\lambda = E\nu/(1 + \nu)(1 - 2\nu)$$

$$\mu = E/2(1 + \nu)$$

The expressions shown in equations 3 satisfy the differential equations of equilibrium (1).

Fracture Formed in an Infinite Medium

A fracture can be formed by continuously injecting a fluid under high pressure through a slotted perforation in a cemented well casing. When the hydraulic pressure in the well reaches a value in excess of the resultant of the rock stresses plus the maximum cohesive forces of the rock, the rock around the well is ruptured and a small fracture is formed in the vicinity of the well. This small fracture, which will be extended after the fluid enters, can be considered a small cut in the massif. Because the fracture extends slowly as the applied pressure is increased gradually, it can be treated as an equilibrium fracture. This kind of fracture has been studied extensively.

To simplify the model, it is assumed that the fracture is formed in an infinite elastic medium and is shaped as a thin disk occupying a circle $r^2 = x^2 + y^2 = a^2$ on the fracture plane, where a is the radius of the fracture.

It is also assumed that the hydraulic pressure p is the only pressure within the induced fracture, and that it is uniformly applied over the entire surface of the fracture. The boundary conditions on the fracture plane are

$$\begin{aligned} \tau_{rz} &= 0 && \text{for all values of } r \\ \sigma_z &= -p && \text{for } r < a \\ W &= 0 && \text{for } r > a \end{aligned} \qquad (4)$$

and all the components of stress tend to zero as $r \to \infty$ or $z \to \infty$. The negative sign on a normal stress denotes compression and the positive sign denotes tension.

The problem of inducing a fracture in an infinite medium has been studied by *Sneddon* [1946] and *Green* [1949]. Sneddon applied the Hankel transform, reducing the problem to the solution of a pair of dual integral equations. Green adopted *Love's* [1939] idea of introducing a complex axis into the system. He conveniently expressed all values of z and r in the stress function $\Phi(r, z)$ in terms of the complex distances R_1 and R_2, which are defined as

$$R_1^2 = r^2 + (z - ia)^2$$

$$R_2^2 = r^2 + (z + ia)^2$$

where, for $z \geq 0$, the arguments of R_1 and R_2 are so chosen that

$$\begin{aligned}
R_1 &= z - ia && \text{for } r = 0\\
R_2 &= z + ia && \text{for } r = 0\\
R_1 &= -i(a^2 - r^2)^{1/2} && \text{for } r \leq a\\
R_1 &= (r^2 - a^2)^{1/2} && \text{for } r \geq a\\
R_2 &= i(a^2 - r^2)^{1/2} && \text{for } r \leq a\\
R_2 &= (r^2 - a^2)^{1/2} && \text{for } r \geq a\\
& && z = 0
\end{aligned} \tag{5}$$

The stress function as derived by *Green* [1949] is

$$\Phi_1(r, z) = \frac{ip(1 + \nu)(1 - 2\nu)}{2\pi E} \cdot \left((2z^2 + 2a^2 - r^2) \log_e \frac{R_2 + z + ia}{R_1 + z - ia} - 3z(R_2 - R_1) + ia(R_2 + R_1)\right) \tag{6}$$

By differentiating $\Phi_1(r, z)$ with respect to z and r, and by using equations 2 and 3, the components of displacement and stress can be calculated. They are

$$U = \frac{ip(1 + \nu)(1 - 2\nu)}{2\pi E}\left[r \log_e \frac{R_2 + z + ia}{R_1 + z - ia} - \frac{r}{2}\left(\frac{ia - 3z - R_2}{R_2 + z + ia} + \frac{R_1 + 3z + ia}{R_1 + z - ia}\right) - \frac{2z^2 r}{1 - 2\nu}\left(\frac{1}{R_2(R_2 + z + ia)} - \frac{1}{R_1(R_1 + z - ia)}\right) + \frac{2zr}{1 - 2\nu}\left(\frac{1}{R_2} - \frac{1}{R_1}\right)\right] \tag{7a}$$

$$W = \frac{2ip(1 - \nu^2)}{\pi E}\left\{z \log_e \frac{R_2 + z + ia}{R_1 + z - ia} - (R_2 - R_1) - \frac{1}{2(1 - \nu)} \cdot \left[z \log_e \frac{R_2 + z + ia}{R_1 + z - ia} - iaz\left(\frac{1}{R_2} + \frac{1}{R_1}\right)\right]\right\} \tag{7b}$$

$$\sigma_z = \frac{ip}{\pi}\left[\log_e \frac{R_2 + z + ia}{R_1 + z - ia} - ia\left(\frac{1}{R_2} + \frac{1}{R_1}\right) - iaz^2\left(\frac{1}{R_2^3} + \frac{1}{R_1^3}\right) + a^2 z\left(\frac{1}{R_2^3} - \frac{1}{R_1^3}\right) - z\left(\frac{1}{R_2} - \frac{1}{R_1}\right)\right] \tag{7c}$$

$$\tau_{rz} = -\frac{ipz}{\pi}\left[r\left(\frac{1}{R_2(R_2 + z + ia)} - \frac{1}{R_1(R_1 + z - ia)}\right) + iar\left(\frac{1}{R_2^3} + \frac{1}{R_1^3}\right)\right] \tag{7d}$$

These components are exactly the same as those found by *Sneddon* [1946, 1951, pp. 229-260], but they are in different mathematical forms.

From the relationships shown in (5), the following expressions are obtained

$$\begin{aligned}
\log_e \frac{R_2 + z + ia}{R_1 + z - ia} &= \log_e \frac{i(a^2 - r^2)^{1/2} + ia}{-i(a^2 - r^2)^{1/2} - ia}\\
&= i\pi \quad \text{for } r < a\\
R_1 &= -R_2 \quad \text{for } r < a\\
R_1 &= R_2 \quad \text{for } r > a\\
& \qquad z = 0
\end{aligned}$$

When the above expressions are substituted into (7), the results are

$$\begin{aligned}
W &= 0 && \text{for } r > a\\
\tau_{rz} &= 0 && \text{for all values of } r
\end{aligned}$$

$$\sigma_z = -p \quad \text{for} \quad r < a$$
$$z = 0$$

which are the boundary conditions.

The stress function $\Phi_1(r, z)$ is a harmonic function that satisfies the equations of equilibrium (1) as well as the boundary conditions.

Calculation of Maximum Separation and Radius of an Induced Fracture in an Infinite Medium

When the relationships shown in (5) are substituted into (7), the result is [*Sneddon*, 1946]

$$W = \frac{4p(1-\nu^2)}{\pi E}(a^2 - r^2)^{1/2}$$
$$\text{for} \quad r < a, \quad z = 0 \qquad (8)$$

The maximum separation of a fracture B should occur at the well site ($r = 0$)

$$B = 2W_{r=0} = \frac{8(1-\nu^2)pa}{\pi E}$$
$$\text{for} \quad r = 0, \quad z = 0 \qquad (9)$$

If Q is the total volume of the injected fluid, then the radius of the fracture a is found as follows [*Perkins and Kern*, 1961]

$$Q = \int_0^a 4\pi W_{z=0}(r\,dr) = \frac{16(1-\nu^2)pa^3}{3E} \qquad (10a)$$

or

$$a = [3EQ/16(1-\nu^2)p]^{1/3} \qquad (10b)$$

Fracture Formed in a Semi-Infinite Medium

Field conditions for hydraulically inducing fractures are different from those assumed in the idealized infinite medium. The hydraulic fracture is formed at a finite distance h below a free ground surface. There is a formation overburden pressure acting on the fracture, which has a tendency to close it. If γ is the average specific weight of the rock plus the contained water, and h is the depth of the fracture below the surface, then the overburden pressure acting on the fracture is γh.

To be meaningful, the theoretical analysis presented above has to be modified for a semi-infinite medium with a free ground surface. Let x, y, and z be coordinates for the infinite

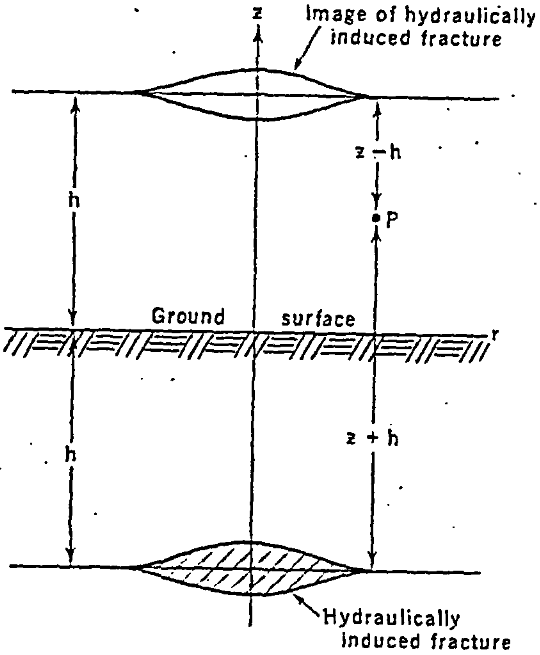

Fig. 1. System for hydraulic fracturing of semi-infinite medium balanced by an image system.

medium with the origin at the center of the fracture, and let x', y', and z be coordinates for the semi-infinite medium with the origin at the ground surface.

The boundary conditions on the x'-y' plane (ground surface) are $\tau_{rz} = \sigma_z = 0$, for all values of r. The normal and shear stresses in an infinite medium on a plane at a distance of h from the fracturing plane can be calculated by substituting $z = h$ and $p = (p - \gamma h)$ into (7). At no point on the $z = h$ plane is τ_{rz} or σ_z equal to zero; yet they should vanish if the boundary conditions on a free surface are to be satisfied.

The image method can be used to bring the system into equilibrium. Equal and opposite hydraulic fracturing conditions are applied at the image plane, as shown in Figure 1. With this method, the horizontal and vertical displacements, and the shear and normal stresses at any point P in the system will be the combined result of both the actual and image hydraulic fracturing pressures. The stresses and displacements can be calculated from (7) by substituting $z = z + h$ for those values of z caused by the actual fracturing pressure, $z =$

$z - h$ for those values affected by the image pressure, and $(p - \gamma h)$ for the injection pressure. By calculation

$$\tau_{rz} = 0 \tag{11a}$$

$$\sigma_z = 2(\sigma_z)_{\text{actual}} = \frac{2i(p-\gamma h)}{\pi}\left[\log_e \frac{R_2 + h + ia}{R_1 + h - ia} - ia\left(\frac{1}{R_2} + \frac{1}{R_1}\right) - h\left(\frac{1}{R_2} - \frac{1}{R_1}\right) - iah^2\left(\frac{1}{R_2^{\,3}} + \frac{1}{R_1^{\,3}}\right) + a^2h\left(\frac{1}{R_2^{\,3}} - \frac{1}{R_1^{\,3}}\right)\right] \tag{11b}$$

Equations 11 show that only the shear stress vanishes at the free ground surface. To satisfy the boundary conditions, however, the normal stress must also vanish. To satisfy the equations of equilibrium and the boundary conditions, it is necessary to introduce a new stress function, which will be a harmonic function and which will yield a normal stress on the ground surface with the value shown by (11*b*) but of opposite sign. To satisfy the desired boundary conditions, the new stress function should not produce any shear stress on the ground surface.

By using (3*b*) and (11*b*), the following relation is found:

$$\frac{\partial^2 \Phi_2}{\partial z^2} = \frac{4i(p-\gamma h)(1+\nu)(1-2\nu)}{\pi E}\left[\log_e \frac{R_1 + h - ia}{R_2 + h + ia} + ia\left(\frac{1}{R_2} + \frac{1}{R_1}\right) + h\left(\frac{1}{R_2} - \frac{1}{R_1}\right) + iah^2\left(\frac{1}{R_2^{\,3}} + \frac{1}{R_1^{\,3}}\right) - a^2h\left(\frac{1}{R_2^{\,3}} - \frac{1}{R_1^{\,3}}\right)\right] \tag{12}$$

$$z = 0$$

It can be verified that

$$\log_e [(R_4 + z - h + ia)/(R_3 + z - h - ia)]$$

$$1/R_4 \qquad 1/R_3$$

$$(z - h + ia)/R_4^{\,3} \qquad (z - h - ia)/R_3^{\,3}$$

are harmonic functions. If

$$\frac{\partial^2 \Phi_2}{\partial z^2} = \frac{4i(p-\gamma h)(1+\nu)(1-2\nu)}{\pi E}\left[\log_e \frac{R_4 + z - h + ia}{R_3 + z - h - ia} - ia\left(\frac{1}{R_4} + \frac{1}{R_3}\right) + h\left(\frac{1}{R_4} - \frac{1}{R_3}\right) + iah\left(\frac{z-h+ia}{R_4^{\,3}} + \frac{z-h-ia}{R_3^{\,3}}\right)\right]$$

then the above expression is also a harmonic function which, at $z = 0$, reduces to (12). The new stress function is obtained by integration of this expression.

$$\Phi_2(r, z) = \frac{i(p-\gamma h)(1+\nu)(1-2\nu)}{\pi E} \cdot \left((2z^2 - 2h^2 + 2a^2 - r^2)\log_e \frac{R_4 + z - h + ia}{R_3 + z - h - ia} + (3z+h)(R_3 - R_4) + ia(R_4 + R_3)\right) \tag{13}$$

By differentiating $\Phi_2(r, z)$ with respect to r, z, and by using equations 2 and 3, the components of displacement and stress produced by this new stress function can be calculated.

The components of stress and displacement induced by the fracturing pressure acting in the interior of the earth at a depth of h with a free ground surface as its boundary can be considered the resultant of the actual and image pressures and the new stress function which mathematically makes the whole system satisfy the boundary conditions at the ground surface.

Calculation of Uplift and Horizontal Movement of the Ground Surface at an Injection Site

Uplift of the ground surface produced by the actual hydraulic fracturing pressure in the subsurface can be determined by (7b)

$$W_{actual} = \frac{2i(p - \gamma h)(1 - \nu^2)}{\pi E} \left\{ h \log_e \frac{R_2 + h + ia}{R_1 + h - ia} - (R_2 - R_1) - \frac{1}{2(1-\nu)} \left[h \log_e \frac{R_2 + h + ia}{R_1 + h - ia} - iah\left(\frac{1}{R_2} + \frac{1}{R_1}\right) \right] \right\}$$

The image-fracturing pressure is symmetrical and opposite to the actual-fracturing pressure. Therefore the uplift produced by the image force is

$W_{image} = -W_{actual}$ at the ground surface

The uplift produced by the new stress function (W_{sf}) can be calculated by using (2b) and (13)

$$W_{sf} = \frac{4i(p - \gamma h)(1 - \nu^2)}{\pi E} \cdot \left[(R_3 - R_4) - iah\left(\frac{1}{R_4} + \frac{1}{R_3}\right) \right] = \frac{4i(p - \gamma h)(1 - \nu^2)}{\pi E} \cdot \left[(R_1 - R_2) + iah\left(\frac{1}{R_1} + \frac{1}{R_2}\right) \right] \tag{14}$$

where

$$R_1^2 = r^2 + (h - ia)^2$$
$$R_2^2 = r^2 + (h + ia)^2$$

The actual uplift of the ground surface is the sum of the three individual components; that is

$$W = W_{actual} + W_{image} + W_{sf} = W_{sf}$$

The horizontal movement of the ground surface can be calculated by the same process used for calculating uplift.

Because at ground surface

$$R_1^2 = r^2 + (h - ia)^2 = K(\cos\theta - i \sin\theta) = Ke^{-i\theta}$$
$$R_2^2 = r^2 + (h + ia)^2 = K(\cos\theta + i \sin\theta) = Ke^{i\theta}$$

where

$$K = [(r^2 + h^2 - a^2)^2 + (2ah)^2]^{1/2}$$
$$K \cos\theta = r^2 + h^2 - a^2$$
$$K \sin\theta = 2ah$$

then

$$R_1 = a\sqrt{k}\,[\cos(\theta/2) - i \sin(\theta/2)]$$
$$R_2 = a\sqrt{k}\,[\cos(\theta/2) + i \sin(\theta/2)] \tag{15}$$
$$\theta = \operatorname{arccot} \frac{r^2 + h^2 - a^2}{2ah}$$

where

$$\sqrt{k} = \left[\left(\frac{r^2}{a^2} + \frac{h^2}{a^2} - 1\right)^2 + \left(\frac{2h}{a}\right)^2\right]^{1/4}$$

By using (9), (14), and (15), the uplift W, and similarly the horizontal movement U, of the ground surface can be expressed as follows

$$W = \frac{8(1 - \nu^2)(p - \gamma h)a}{\pi E} \left(\sqrt{k} \sin(\theta/2) - \frac{h}{a\sqrt{k}} \cos(\theta/2) \right) = B\left(\sqrt{k} \sin(\theta/2) - \frac{h}{a\sqrt{k}} \cos(\theta/2) \right) \tag{16}$$

$$U = \frac{Brh}{a} \left\{ \frac{(a + a\sqrt{k} \sin(\theta/2))}{[(h + a\sqrt{k} \cos(\theta/2))^2 + (a + a\sqrt{k} \sin(\theta/2))^2]} - \frac{(h\sqrt{k} \cos(\theta/2) - a\sqrt{k} \sin(\theta/2) + ak \cos\theta)}{[(h\sqrt{k} \cos\frac{\theta}{2} - a\sqrt{k} \sin\frac{\theta}{2} + ak \cos\theta)^2 + (a\sqrt{k} \cos\frac{\theta}{2} + h\sqrt{k} \sin\frac{\theta}{2} + ak \sin\theta)^2]} \right\} \tag{17}$$

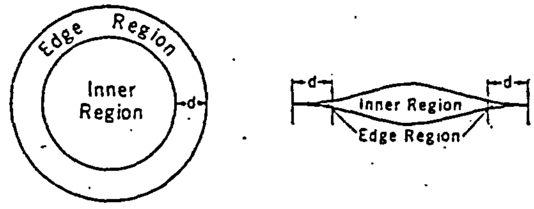

Fig. 2. Two regions of a fracture.

Before (16) and (17) can be applied, it is necessary to determine whether the equations for calculating the maximum separation and radius of a fracture (equations 9 and 10) are still valid for a fracture formed in a semi-infinite medium. The effect of the free ground surface on the separation and radius of a fracture formed in the subsurface has been studied by using (2), (6), and (12). It was found that if $5ah \geq 2a$, the influence is only about 2 to 3%. If $h \geq 5a$, the influence is almost zero. *Ustinov* [1959] found the same results by using a different method. Therefore it was concluded that (9) and (10) can be used to determine the maximum width and radius of a fracture formed in the interior of the earth disregarding the effects of the free ground surface.

If the average injection pressure in the fracture and the volume of the injected material are known, the radius of the fracture can be calculated from (10), which is derived from (7b), for equilibrium conditions. However, analysis of (7) shows that there is an infinite tensile stress at the edge of the fracture (where $r = a$). Consequently it is concluded that an equilibrium fracture cannot exist.

Before any modifications are made in the formulas used for calculating the maximum separation and radius of the fracture (equations 9 and 10), it is necessary to consider further the mechanism of extending an existing fracture in a brittle material. During the process of extension, the increased pressure in the fracture separates the material into two parts along the fracture plane from the pre-existing equilibrium position, but there is a molecular attraction that resists the separation according to the law of cohesion. The intensity of the force of cohesion depends mostly on the distance of separation of neighboring molecular planes.

When the pressure in an existing fracture is increased, the material at the edge of the fracture begins to separate. When the applied force in the fracture overcomes the maximum cohesive force acting on the separating surface near the edge of the fracture, the fracture starts to extend. The applied force in the fracture is balanced by the total cohesive force.

Griffith [1921] was first to analyze the cohesive forces of molecules on both sides of a fracture. He considered these cohesive forces as forces of surface tension that must be overcome when the fracture is extended. Griffith neglected the effect of the cohesive forces on the stress and strain field.

Barenblatt [1962] considered the cohesive forces in more detail. He divided the fracture into two regions. In the inner region the opposite faces of the fracture are relatively far apart; hence there is no molecular interaction between them, and the fracture surface can be considered free of stresses. In the edge region of width d (Figure 2), the opposite faces of the fracture are sufficiently close to each other so that there are strong cohesive forces between them, which must be taken into account in calculating the separation and radius of the fracture. To avoid a very complex nonlinear integral equation and to simplify the problem, Barenblatt made the following assumptions:

1. The width of the edge region of the fracture is small when compared with the size of the whole fracture.
2. When the fracture extends, the shape of the section normal to the fracture surface in the edge region (and consequently the local distribution of the cohesive force over the fracture surface) does not depend on the pressure in the fracture and is always the same for a given material under given conditions of temperature and overburden pressure.

From these assumptions, *Barenblatt* [1962, p. 74] proved mathematically that a fracture has the following significant characteristics:

1. The tensile stress at the ends of a fracture is finite; if there are no cohesive forces, the tensile stress at the fracture ends is equal to zero.
2. The opposite faces of a fracture meet gradually at the ends.

Barenblatt also stated that, as the pressure in the fracture increases, cohesive forces in the edge region also increase; they compensate for the increase in the load, thus ensuring that the tensile stress is finite and that the fracture surfaces meet gradually. However, the fracture does not extend until the cohesive forces reach a maximum. The influence of cohesive forces on the stress and displacement field is significant only in the neighborhood of the edge region.

The formula given above (equation 10) for determining the radius of a fracture is based on Sneddon's and Green's works, which are the extension of Griffith's fracture theory, and ignores the effect of cohesive forces on the stress and strain field near the edge region of a fracture. A more accurate value for the radius of a fracture can be calculated by taking into consideration the fracture shape derived by *Barenblatt* [1962]. In his conception of a fracture the separation of the opposite faces at the edge region is very small and is regarded as a strain rather than as a displacement. Therefore part of the space within the edge region is still occupied by the formation fluid instead of the injection fluid. In comparison with the overburden pressure of rock and the injection pressure, the forces of cohesion are so small that they may be neglected [*Barenblatt*, 1962, p. 112]. Under these circumstances the boundary conditions need to be modified as shown in Figure 3 [*Barenblatt*, 1956].

$$\sigma_z = -(p - \gamma h) \quad \text{for} \quad 0 \leq r \leq a$$

$$\sigma_z = \gamma h \quad \text{for} \quad a \leq r \leq a'$$

$$z = -h$$

By these boundary conditions and the condition of finiteness of stresses at the contour of a horizontal fracture, the following relation is found [*Barenblatt*, 1956, 1962; *Zheltov and Khristianovich*, 1955]

$$(1 - \alpha^2)^{1/2} = (p - \gamma h)/p \qquad (18)$$

where

$$\alpha = a/a'.$$

If the pressure $(p_0 - \gamma h)$ is assumed to be uniformly distributed over the entire fracture areas with a radius of a, where p_0 is the injection pressure at the bottom of the well, then the average pressure over the entire circular area with a radius of a' can be assumed approximately as $\alpha^2 (p_0 - \gamma h)$. In this case, the boundary conditions of (4) can be changed as

$$\tau_{rz} = 0 \qquad \text{for all values of } r$$

$$\sigma_z = -\alpha^2(p_0 - \gamma h) \quad \text{for} \quad r < a'$$

$$W = 0 \qquad \text{for} \quad r > a'$$

Therefore (9) and (10) can be rewritten as

$$B = 8(1 - \nu^2)(p_0 - \gamma h)\alpha^2 a'/\pi E \qquad (19)$$

$$a' = \frac{a}{\alpha} = \left(\frac{3EQ}{16(1 - \nu^2)\alpha^6(p_0 - \gamma h)}\right)^{1/3} \qquad (20)$$

The uplift and horizontal movement of the ground surface produced by the hydraulic fracturing can be calculated by (16), (17), (19), and (20) and by substituting values of a' for a in (16) and (17).

Hydraulic Fracturing at Oak Ridge National Laboratory, Tennessee

The hydraulic fracturing experiments, conducted at ORNL from 1960 to 1965 to evaluate the feasibility of disposing of radioactive waste by injecting grout mixtures into shale, provided an opportunity for comparing the theoretical size of hydraulically induced fractures and corresponding surface uplift in an idealized medium, with field measurements at the injection sites.

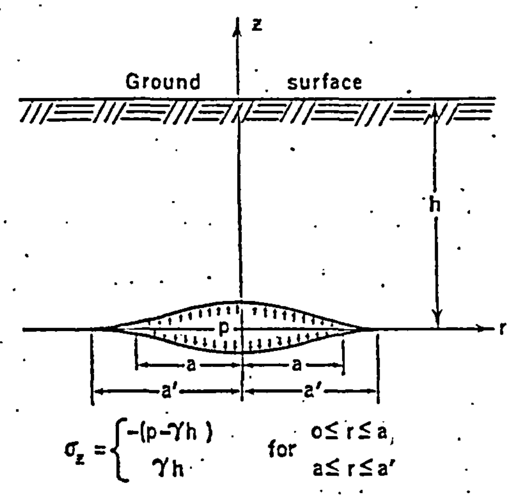

Fig. 3. Modified boundary conditions for a fracture formed in a semi-infinite medium.

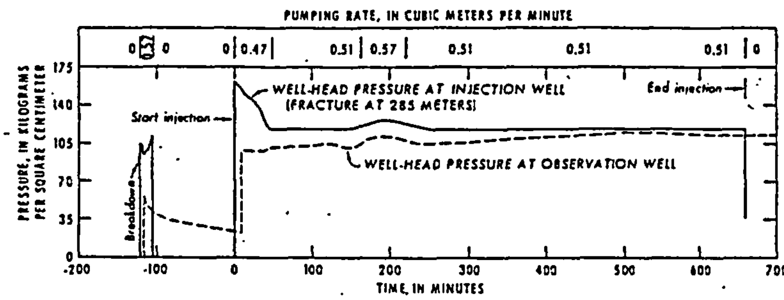

Fig. 4. Pressure history of the injection of September 3, 1960 [after *DeLaguna et al.*, 1968].

Geologic conditions. ORNL is located in the Appalachian belt of faulted and folded Paleozoic rocks. Four major formations underlie the general area; in ascending order, they are the Knox group (dolomite), the Chickamauga limestone, the Rome formation (sandstone), and the Conasauga shale. The Conasauga shale is about 300 meters thick at the hydraulic fracturing site. All the injections have been made into the lowermost unit of the Conasauga shale, the Pumpkin Valley member. It is a dominantly red, dense, argillaceous, very thin-bedded shale, about 90 meters thick. The permeability of the Conasauga shale is very low, about 10^{-4} millidarcy [*DeLaguna*, 1966, Figure 2].

A series of great overthrust faults has been mapped in the vicinity of the injection sites. All the formations dip to the southeast about 45° at the outcrops of the overthrust faults, but they flatten out southeast of the faults to 10° to 20° [*DeLaguna*, 1966]. At the injection site of the third experiment, however, the expected 20° dip was not found. Rather, the logs of the wells showed that identifiable geologic formations occurred at about the same depth at the injection well as at an observation well 46 meters north of the injection well [*DeLaguna et al.*, 1963].

Comparison between calculations and field measurements. Data from two surveyed uplifts from the injection of grout sheets in the second experiment, September 3 and 10, 1960 [*DeLaguna*, 1966], together with data from three surveyed uplifts produced by seven injections of the third experiment, February 1964 through August 1965 [*DeLaguna et al.*, 1968], were used for testing the validity of the mathematical model for calculating uplift. Calculations of the areal extent and maximum separation of fractures for the two injections of the second experiment were made for comparison with data obtained by coring the grout sheets.

The calculation of the size of fracture resulting from the September 3, 1960, injection of the second experiment is considered typical and is presented as a sample.

This injection was made through a slot in the casing at a depth of 285 meters and consisted of 346 m³ (91,500 gallons) of grout containing 201 tons of cement and 5700 kg of bentonite clay 'tagged' with 25 curies of cesium 137 [*DeLaguna and Jacobs*, 1961]. Fracturing was initiated with water. The well was 'broken down' (fracturing started) at 106 kg/cm² of pressure at the surface; then the pressure fell quickly to 95 kg/cm² at a pumping rate of 0.57 m³/min and increased to 115 kg/cm² as the rate was increased slightly. Six minutes after the fracture was started, by which time 3.2–3.4 m³ of water had been pumped, the pressure in the nearby observation well, 9 meters west of the injection well, suddenly rose to 56 kg/cm², indicating that the fracture had extended into it. After the pump was stopped, the water was bled back out of the injection well, and the pressure in the observation well fell to 25 kg/cm² in about 100 min. The main injection of water-cement-bentonite mixture was then started. The maximum pressure for the slurry injection was about 162 kg/cm²; about 40 min after the injection started, the pressure dropped to 120 to 123 kg/cm² [*DeLaguna*, 1966]. The history of pressure as related to the pumping rate and time during the injection is shown in Figure 4.

The physical properties of the slurry are described in Table 1. The physical properties of the shale at the test site were not determined during the tests. Data on rock properties used for the calculations were taken from the available literature.

The bulk density of shale in the Appalachian area is about 2.7 g/cm³ [*Heck*, 1960; *DeLaguna*, 1966]. Young's modulus E may be taken as 1.83×10^5 kg/cm² and Poisson's ratio ν as 0.10 [*Birch*, 1966, p. 167].

The water injection data were interpreted first. Because the surface injection pressure varied from 95 to 115 kg/cm², owing to the variable pumping rate, the arithmetic average, 105 kg/cm², was used as the mean injection pressure.

The static head of the water in the well casing is

$$p_h = 0.1 \times 285 = 28.5 \text{ kg/cm}^2$$

Since the viscosity of water is low, the frictional head loss in the casing can be neglected and the bottom-hole pressure of the water injection is simply

$$p_0 = 105 + 28.5 = 134 \text{ kg/cm}^2$$

The overburden pressure is

$$\gamma h = 2.7 \times 0.1 \times 285 = 77 \text{ kg/cm}^2$$

The bottom-hole pressure is about 56 kg/cm² greater than the overburden pressure, suggesting that the hydraulically formed fracture may be horizontally oriented. By using (18) and (20), and the average injection volume of 3.3 m³ (875 gallons), the radius of the fracture can be calculated as follows

$$(1 - \alpha^2)^{1/2} = (134 - 77)/134$$

$$\alpha = 0.905$$

TABLE 1. Physical Properties of Slurries Injected in the Second Experiment, September 1960

Data from J. M. Stogner (personal communication, June 8, 1966, Halliburton Co., Duncan, Oklahoma).

Injection number	1	2
Injection date	Sept. 3	Sept. 10
Density, g/cm³	1.38	1.44
Plastic viscosity, cp	3.000	1.500
Yield point, g/cm³	0.317	0.464
N'	0.109	0.065
K', kg sec$^{N'}$/cm²	163×10^{-6}	303×10^{-6}

TABLE 2. Observed Data on Injections of the Second Experiment, September 1960

Data from *DeLaguna and Jacobs* [1961] and J. M. Stogner (personal communication, June 8, 1966).

Injection number	1	2
Injection date	Sept. 3	Sept. 10
Injection depth, meters	285	212
Outside diameter of casing of the injection well, cm	12	12
Inside diameter of casing of the injection well, cm	10.4	10.4
Average injection rate, m³/min	0.53	0.95
Total injection volume, m³	346	503
Breakdown pressure at well head, kg/cm²	162	155
Injection pressure at well head, kg/cm²	120–141 (average 130)	141–162 (average 152)
Maximum thickness of grout, cm	0.76	1.22

$$a' = \left(\frac{3 \times 3.3 \times 1.83 \times 10^5}{16(1-0.10^2) \times (0.905)^6 \times (134-77)}\right)^{1/3}$$

$$= 15 \text{ meters}$$

$$a = \alpha a' = 13.6 \text{ meters}$$

The horizontal distance between the bottom of the observation well and the bottom of the injection well is uncertain, but it is probably of the order of 6 to 12 meters [*DeLaguna*, 1966]. After 3.2 to 3.4 m³ of water had been injected, the bottom hole pressure in the observation well was 84 kg/cm², which was 7 kg/cm² more than the overburden pressure. This suggests that the fracture had extended beyond the observation well.

For the interpretation of the grout injection data, it is necessary to take into account the fact that grout, composed of bentonite and cement, is a non-Newtonian liquid. The Reynold's number and frictional head loss for non-Newtonian flow through a casing can be calculated by the following formula [*Slagle*, 1962]

$$Re = \frac{8.16 \times 10^{-2} v^{2-N'} \rho}{K'(800/D)^{N'}}$$

$$\Delta p = 2.04 L \rho v^2 f / D$$

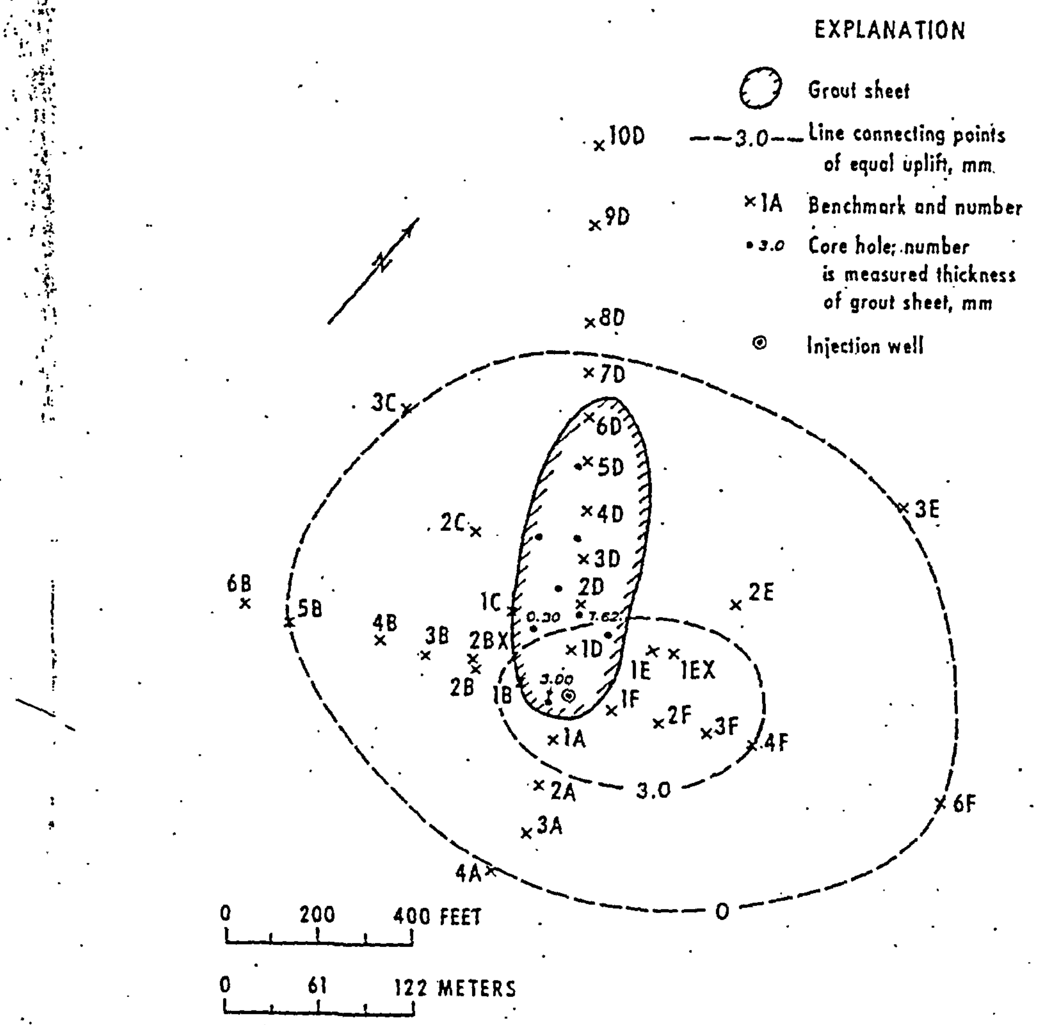

Fig. 5. Surface uplift, extent, and thickness of the grout sheet of the injection of September 3, 1960 [after *DeLaguna et al.*, 1968, and W. DeLaguna (written communication, ORNL, June 10, 1968)].

$f = 16/Re$ for Laminar flow when $Re <$ 2100.

$f = 0.00454 + 0.645\,(Re)^{-0.7}$ for transitional and turbulent flow.

(See nomenclature for definition of terms.) By substituting the data shown in Tables 1 and 2 into the above equation, the Reynold's number and frictional head loss are calculated to be

$$Re = \frac{8.16\times10^{-2}\times(1.04)^{2-0.109}\times1.38}{163\times10^{-6}(800/10.4)^{0.109}} = 463$$

$$\Delta p = \frac{2.04\times285\times1.38\times(1.04)^{2}\times0.0346}{10.4}$$

$$= 3.0\ \mathrm{kg/cm^2}$$

The static head of the slurry in the injection well is

$$P_A = 1.38 \times 0.1 \times 285 = 39\ \mathrm{kg/cm^2}$$

The recorded well-head injection pressure [illegible] 130 kg/cm². Then, the bottom-hole pressure [illegible] acting on the rock surface at the bottom [illegible] the well, is

$$P_0 = 130 + 39 - 3 = 166\ \mathrm{kg/cm^2}$$

The overburden pressure is 77 kg/cm². Th[illegible] fact that the bottom-hole pressure is more th[illegible] double the overburden pressure suggests that the fracture could be horizontal.

By using (18), (19), and (20), the maximum separation and radius of the fracture can be calculated

$$\alpha = 0.844$$

$$a' = \left(\frac{3\times 346\times 1.83\times 10^{5}}{16(1-0.10^{2})\times(0.844)^{5}\times(166-77)}\right)^{1/3}$$

$$= 68 \text{ meters}$$

$$a = \alpha a' = 57.4 \text{ meters}$$

$$B = \frac{8(1-0.10^{2})\times 68\times(0.844)^{2}\times(166-77)}{\pi\times 1.83\times 10^{6}}$$

$$= 5.94 \text{ cm}$$

Core-hole data on the extent and thickness of the grout sheet of the first injection, second experiment, are shown in Figure 5; 24 core holes were drilled in this area. Only the holes that intersected the grout sheets are shown on this map and on Figure 6, which shows the grout sheet from the second injection. It appears that the injected grout moved generally toward the north and assumed an elliptical

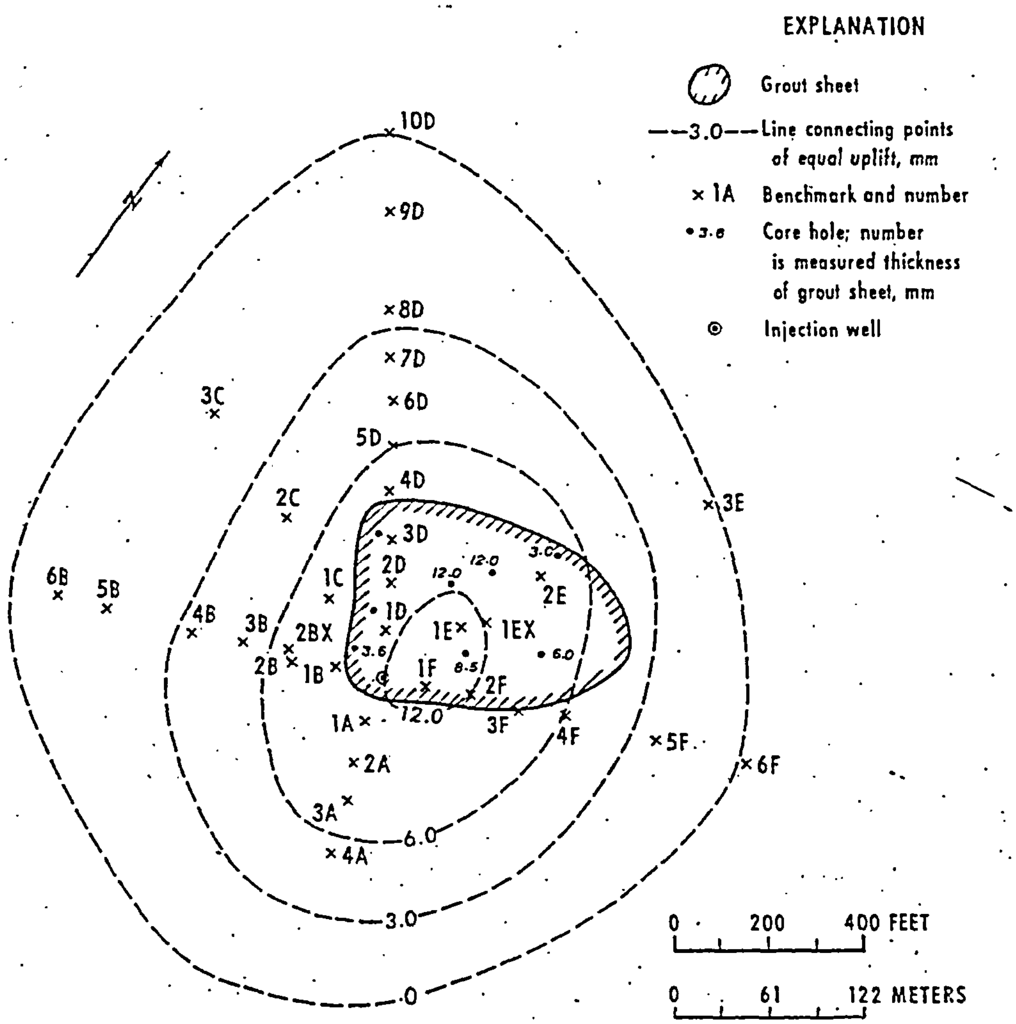

Fig. 6. Surface uplift, extent, and thickness of the grout sheet of the injection of September 10, 1960 [after *DeLaguna et al.*, 1968, and W. DeLaguna (written communication, ORNL, June 10, 1968)].

TABLE 3. Calculated Maximum Separation and Radius of Fractures Produced by Injections of the Second Experiment, September 1960

Injection number	1	2
Injection date	Sept. 3	Sept. 10
Area of casing, cm^2	85	85
Velocity of slurry, m/sec	1.04	1.86
Re	463	970
Total friction loss, kg/cm^2	3.0	4.0
Static pressure of slurry in the well casing, kg/cm^2	39	31
Injection pressure at bottom of the well (p_0), kg/cm^2	166	179
Overburden pressure (γh), kg/cm^2	77	57
α	0.844	0.732
$\alpha^2(p_0 - \gamma h)$, kg/cm^2	64	65
Calculated maximum radius of the stress-altered region (a'), meters	68	88
Calculated radius of grout (a), meters	57	64
Calculated maximum separation of fracture (B), cm	5.94	7.92

shape. No relation could be found between the areal shape of the grout sheet and the pattern of uplift. The cored grout sheet of the second injection (September 10, 1960) appears to have a more nearly circular shape, and there seems to be a better correlation with the uplift pattern (Figure 6). However, there is no satisfactory explanation for the apparent movement of the grout sheets north from the injection well. It is suggested that the true shape of the grout sheets is much more irregular in outline, and that this is part of the reason for the apparently poor correlation between their shape and the pattern of uplift. In view of the fact that in each case the center of the grout sheet was offset with respect to the injection well, there is no way to compare the calculated maximum radius with the actual radius of the sheet. The calculated values of these grout sheets are given in Table 3 along with related data used in the calculations.

The uplift and horizontal movement of the ground surface produced by the injection can be calculated from (16) and (17) by substituting the value a' for a. The horizontal movement of the ground surface is apparently very small and can be neglected. The comparison between the calculated and surveyed uplift is shown graphically in Figures 7, 8, and 9. Generally speaking, the calculated results are in good agreement with the observed data.

The maximum thickness of the grout sheets as measured in cores is much less than the calculated maximum separation of the fractures (Figures 5 and 6 and Table 3). This is not surprising in view of the fact that the liquid phase of the injected slurry probably was squeezed out and the solid phase compacted by the overburden pressure. The grout in the cores appeared to be nearly as hard as the shale into which it has been injected. Unfortunately, no data are available on the compaction of such slurries; otherwise, it would be interesting to compare the thickness of the cored grout sheets with the calculated figures of fracture separation.

Records from oil well fracturing operations do, however, permit a comparison of the calculated separation of hydraulically induced horizontal fractures in the vicinity of an oil well with the observed separation in an adjacent core hole by an impression-packer (latex-coated packer) survey. Oil well Reno 20 Q, which is located 152 meters north of 41°25'N and 762 meters east of 79°45'W in the Reno oil field, Venango County, Pennsylvania, was hydraulically fractured in three stages by the Quaker State Oil Refining Corporation. The strata involved in the fracturing operations included a thin layer of sandstone with considerable variation in texture and thickness, between thick

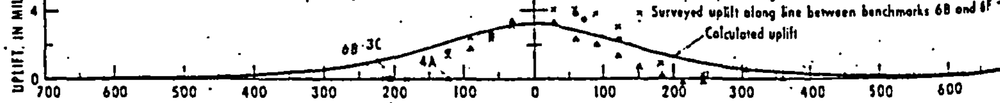

Fig. 7. Calculated and surveyed uplift produced by injection 1, second experiment, September 3, 1960.

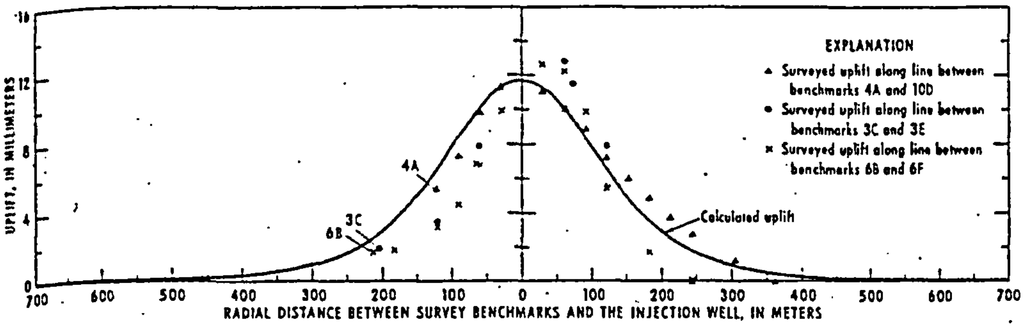

Fig. 8. Calculated and surveyed uplift produced by injection 2, second experiment, September 10, 1960.

locally silty shale units. After fracturing, impression-packer surveys were made in a core hole (TCW 5) 4½ meters from the injected oil well (Reno 20 Q). The packer surveys indicated that fractures were induced horizontally. The aggregate separation of three or more fractures in the core hole is 2.78 to 2.94 cm, a value that is about 25% smaller than the calculated separation, 3.66 cm. Some of the difference between the observed and calculated separations may stem from the use of average values of the elastic parameters rather than those of specific beds.

Discussion and Conclusions

During the development of the mathematical model, it was thought that the assumption of isotropic, homogeneous, and elastic conditions might not apply to heterogeneous shale formations. As shown by the available data (specifically the calculated and surveyed surface uplift produced by the grout injections), however, this assumption appears to be generally valid.

The shale formation at the ORNL site seems to react as an elastic body because the uplift produced by the injections in 1960 (second experiment) had subsided and the ground surface had returned to its original elevation, as indicated by a resurvey of the area in 1964 [*De-Laguna*, 1966, p. 434, Figure 2]. Also, a level survey conducted in May 1965, about one year after the fifth injection of the third experiment, showed that with only a few exceptions the elevation of all benchmarks had subsided by a small amount.

An analysis of (19) and (20) shows that the radius of a hydraulically induced fracture is inversely proportional to the cube root of the injection pressure, but the amount of separation of the fracture is directly related to the pressure. The relation between fracture separation and pressure can be explained by the fact that use of a viscous fluid and/or a high injection rate, which usually results in high injection pressure, requires a large flow channel to reduce the frictional head loss; therefore the separation

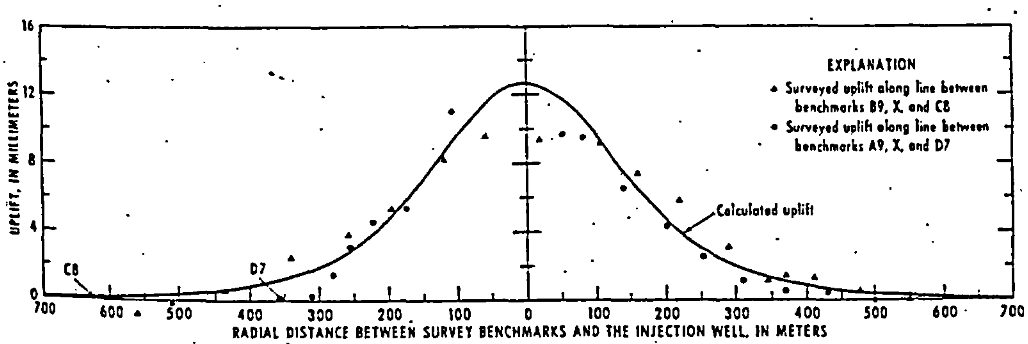

Fig. 9. Calculated and surveyed uplift produced by injections 3, 4, and 5, third experiment, April 8 and 17 and May 28, 1964.

of a fracture induced under these conditions should be greater than that for a less viscous fluid or for a small injection rate. For a water injection, the separation of the fracture should be small, resulting in a small amount of uplift and therefore requiring highly precise surveys to measure the amount of uplift of the ground surface.

It appears feasible, at least for conditions similar to those at ORNL, to deduce the orientation of a hydraulically induced fracture from the injection data. Equation 19 shows that for a horizontal fracture the bottom-hole pressure at the injection well during the injection period must exceed the overburden pressure; otherwise, the fracture will be vertical or steeply inclined, or the formation will not be fractured. If the fracture is horizontal, the ground surface should be uplifted by an amount that can be calculated and checked by a level survey.

The calculated amount of uplift agrees reasonably well with the survey data available for this report, but, for further validation of the theory, more precise data are required. Such data should include physical properties of rocks and injection fluid, formation fluid pressure, rock permeability, bottom-hole injection pressure (a constant pressure is recommended), and uplift of the ground surface (surveys with accuracy better than first-order levels are highly recommended). Also, measurements of the horizontal movement of the land surface are needed to determine the validity of the calculated data.

Acknowledgments. This work was sponsored by the U. S. Atomic Energy Commission and was undertaken at the request of Mr. W. G. Belter, Chief, Environmental and Sanitary Engineering Branch, Division of Reactor Development and Technology. The cooperation of Mr. E. G. Struxness, ORNL, and Dr. F. L. Parker, ORNL (presently professor at Vanderbilt University, Nashville, Tennessee), is gratefully acknowledged. I wish to thank my colleagues, Messrs. W. O. Smith and E. L. Meyer, for many profitable discussions on various aspects of the problem. I am grateful to Drs. C. V. Theis, B. F. Grossling, and C. E. Mongan, and to Mr. Robert Schneider, for their review and constructive criticism; they are in no way responsible for any errors or misinterpretations that may be present in the paper. I am especially indebted to Drs. Wallace DeLaguna, W. C. McClain, and Tsuneo Tamura (ORNL); to Mr. J. M. Stogner (Halliburton Co.), and to Mr. G. M. Wiesner (Quaker State Oil Refining Corp.) for providing supporting data. Publication authorized by the Director, U.S. Geological Survey.

References

Barenblatt, G. I., Facing some problems of theory of elasticity, during investigation of the mechanism of hydraulic fractures of oil-bearing formation (in Russian), *Izv. Akad. Nauk SSSR Inst. Mekh.*, *20*, 475–486, 1956.

Barenblatt, G. I., The mathematical theory of equilibrium cracks in brittle fracture, in *Advances in Applied Mechanics*, edited by H. L. Dryden and Th. Von Karman, pp. 55–129, Academic Press, New York, 1962.

Birch, F., Compressibility, elastic constant, in *Handbook of Physical Constants, Section 7* (revised edition), edited by S. P. Clark, Jr., 587 pp., *Geol. Soc. Amer. Mem.*, *97*, 1966.

Clark, J. B., A hydraulic process for increasing the productivity of wells, *Trans. AIME*, *186*, 1–8, 1949.

Cleary, J. M., Hydraulic fracture theory, 1, *Mechanics of Materials, Ill. State Geol. Surv. Circ. 251*, 24 pp., 1958a.

Cleary, J. M., Hydraulic fracture theory, 2, *Fracture Orientation and Possibility of Fracture Control, Ill. State Geol. Surv. Circ. 252*, 19 pp., 1958b.

Crittendon, R. C., The mechanics of design and interpretation of hydraulic fracture treatments, *J. Petrol. Technol.*, 21–29, October 1959.

Dean, W. R., H. W. Parsons, and I. N. Sneddon, A type of stress distribution on the surface of a semi-infinite elastic solid, *Proc. Cambridge Phil. Soc.*, *40*, 1, 5–18, 1944.

DeLaguna, W., and D. G. Jacobs, Disposal in deep wells, *Oak Ridge Nat. Lab. Ann. Prog. Rep. ORNL 3189*, 69–72, 1961.

DeLaguna, W., T. Tamura, et al., Disposal by hydraulic fracturing, *Oak Ridge Nat. Lab. Ann. Progr. Rept. ORNL-3492*, 13–18, 1963.

DeLaguna, W., Disposal of radioactive wastes by hydraulic fracturing, *Nucl. Eng. Design*, *3*, 338–352 and 432–438, 1966.

DeLaguna, W., E. G. Struxness, et al., Engineering development of hydraulic fracturing as a method for permanent disposal of radioactive wastes, *Oak Ridge Nat. Lab. Rep. ORNL-4259*, 1968.

Fraser, C. D., and B. E. Pettitt, Results of a field test to determine the type and orientation of a hydraulically induced formation fracture, *J. Petrol. Technol.*, 463–466, May 1962.

Green, A. E., On Boussinesq's problem and penny-shaped cracks, *Proc. Cambridge Phil. Soc.*, *45*, 2, 251–257, 1949.

Griffith, A. A., The phenomena of rupture and flow in solids, *Trans. Roy. Soc. London, A*, *221*, 163–198, 1921.

Harrison, E., W. F. Kieschnick, Jr., and W. J. McGuire, The mechanics of fracture induction and extension, *Trans. AIME*, *201*, 252–263, 1955.

Heck, E. T., Hydraulic fracturing in light of geologic conditions, *Prod. Mon.*, *24*(11), 12–13, 16–19, 1960.

Hubbert, M. K., Mechanical bases for certain familiar geologic structures, *Bull. Geol. Soc. Amer.*, *62*(4), 355–372, 1951.

Hubbert, M. K., and D. G. Willis, Mechanics of hydraulic fracturing, *Trans. AIME*, *210*, 153–168, 1957.

Lamont, N., and F. W. Jessen, The effects of existing fractures in rocks on the extension of hydraulic fractures, *Trans. AIME*, *228*, 203–209, 1963.

Love, A. E. H., *A Treatise on the Mathematical Theory of Elasticity*, 4th ed., 643 pp., Cambridge University Press, London, 1934.

Love, A. E. H., Boussinesq's problem for a rigid cone, *Quart. J. Math.*, *10*, 161–175, 1939.

McClain, W. C., T. Tamura, and F. S. Brinkley, Disposal by hydraulic fracturing, *Oak Ridge Nat. Lab. Ann. Progr. Rep. ORNL-4007*, 10–14, 1966.

Odé, H., A note concerning the mechanism of artificial and natural hydraulic fracture system, Symposium on rock mechanics, *Quart. Col. School Mines*, *51*(3), 19–29, 1956.

Perkins, T. K., and L. R. Kern, Width of hydraulic fractures, *J. Petrol. Technol.*, 937–949, September 1961.

Slagle, K. A., Rheological design of cementing operations, *J. Petrol. Technol.*, 323–328, March 1962.

Sneddon, I. N., The distribution of stress in the neighborhood of a crack in an elastic solid, *Proc. Roy. Soc. London, A*, *187*, 229–260, 1946.

Sneddon, I. N., *Fourier Transformations*, 542 pp., McGraw-Hill, New York, 1951.

Timoshenko, S., and J. N. Goodier, *Theory of Elasticity*, 2nd ed., 506 pp., McGraw-Hill, New York, 1951.

Ustinov, Yu. A., On the influence of the free boundary of a half space on the fracture propagation (in Russian), *Izv. Akad. Nauk SSSR Mekhan. Mashinostr.*, *4*, 181–183, 1959.

Zheltov, Yu. P., and S. A. Khristianovich, The hydraulic fracturing of an oil-producing formation (English translation, *Ass. Tech. Serv. RJ-742*), *Izv. Akad. Nauk SSSR Mekhan. Mashinostr.*, *6*, 3–41, 1955.

(Received April 1, 1969;
revised July 30, 1969.)

ATTACHMENT C

Super CBL® and Microbond®
MATERIAL SAFETY DATA SHEETS

HALLIBURTON

MATERIAL SAFETY DATA SHEET

Product Trade Name: **SUPER CBL ADDITIVE**

Revision Date: 07/17/2002

1. CHEMICAL PRODUCT AND COMPANY IDENTIFICATION

Product Trade Name:	SUPER CBL ADDITIVE
Synonyms:	None
Chemical Family:	Metal Powder
Application:	Additive
Manufacturer/Supplier	Halliburton Energy Services P.O. Box 1431 Duncan, Oklahoma 73536-0431 Emergency Telephone: (800) 666-9260 or (713) 676-3000
Prepared By	Product Stewardship Telephone: 1-580-251-4335

2. COMPOSITION/INFORMATION ON INGREDIENTS

SUBSTANCE	CAS Number	PERCENT	ACGIH TLV-TWA	OSHA PEL-TWA
Aluminum	7429-90-5	60 - 100%	5 mg/m^3	15 mg/m^3

3. HAZARDS IDENTIFICATION

Hazard Overview May cause eye and respiratory irritation. May cause delayed injury to lungs. Airborne dust may be explosive.

4. FIRST AID MEASURES

Inhalation If inhaled, remove from area to fresh air. Get medical attention if respiratory irritation develops or if breathing becomes difficult.

Skin Wash with soap and water. Get medical attention if irritation persists.

Eyes In case of contact, immediately flush eyes with plenty of water for at least 15 minutes and get medical attention if irritation persists.

Ingestion Under normal conditions, first aid procedures are not required.

Notes to Physician Not Applicable

5. FIRE FIGHTING MEASURES

Flash Point/Range (F):	Not DeterminedMin: 350
Flash Point/Range (C):	Not DeterminedMin: 176
Flash Point Method:	Not Determined
Autoignition Temperature (F):	1202
Autoignition Temperature (C):	650
Flammability Limits in Air - Lower (%):	0.04
Flammability Limits in Air - Upper (%):	Not Determined

Fire Extinguishing Media Sand. Do NOT use water or carbon dioxide or other liquids on aluminum fires.

Special Exposure Hazards Flammable dust when in finely divided and highly suspended state. Avoid stirring burning aluminum. Shut off electricity. Isolate material. Ring sand around fire to contain.

Special Protective Equipment for Fire-Fighters Full protective clothing and approved self-contained breathing apparatus required for fire fighting personnel.

NFPA Ratings: Health 0, Flammability 1, Reactivity 1
HMIS Ratings: Flammability 1, Reactivity 1, Health 0

6. ACCIDENTAL RELEASE MEASURES

Personal Precautionary Measures Use appropriate protective equipment. Avoid creating and breathing dust.

Environmental Precautionary Measures None known.

Procedure for Cleaning/Absorption Remove ignition sources and work with non-sparking tools. Scoop up and remove.

7. HANDLING AND STORAGE

Handling Precautions Avoid creating or inhaling dust.

Storage Information Store away from oxidizers. Store away from acids. Store away from alkalis. Store away from water. Store in a cool, dry location.

8. EXPOSURE CONTROLS/PERSONAL PROTECTION

Engineering Controls Use in a well ventilated area.

Respiratory Protection Dust/mist respirator. (95%)

Hand Protection Normal work gloves.

Skin Protection Normal work coveralls.

Eye Protection Wear safety glasses or goggles to protect against exposure.

Other Precautions None known.

9. PHYSICAL AND CHEMICAL PROPERTIES

Physical State:	Solid
Color:	Silver
Odor:	Odorless

pH:	Not Determined
Specific Gravity @ 20 C (Water=1):	2.7
Density @ 20 C (lbs./gallon):	Not Determined
Bulk Density @ 20 C (lbs/ft3):	72
Boiling Point/Range (F):	Not Determined
Boiling Point/Range (C):	Not Determined
Freezing Point/Range (F):	Not Determined
Freezing Point/Range (C):	Not Determined
Vapor Pressure @ 20 C (mmHg):	Not Determined
Vapor Density (Air=1):	Not Determined
Percent Volatiles:	Not Determined
Evaporation Rate (Butyl Acetate=1):	Not Determined
Solubility in Water (g/100ml):	Insoluble
Solubility in Solvents (g/100ml):	Not Determined
VOCs (lbs./gallon):	Not Determined
Viscosity, Dynamic @ 20 C (centipoise):	Not Determined
Viscosity, Kinematic @ 20 C (centistrokes):	Not Determined
Partition Coefficient/n-Octanol/Water:	Not Determined
Molecular Weight (g/mole):	Not Determined

10. STABILITY AND REACTIVITY

Stability Data:	Stable
Hazardous Polymerization:	Will Not Occur
Conditions to Avoid	Keep away from any contact with water.
Incompatibility (Materials to Avoid)	Contact with water. Strong acids. Strong alkalis. Strong oxidizers. Halogenated compounds.
Hazardous Decomposition Products	Flammable hydrogen gas. Metal oxides.
Additional Guidelines	Not Applicable

11. TOXICOLOGICAL INFORMATION

Principle Route of Exposure	Eye or skin contact, inhalation.
Inhalation	May cause respiratory irritation.
Skin Contact	None known.
Eye Contact	May cause mild eye irritation.
Ingestion	None known
Aggravated Medical Conditions	Lung disorders.
Chronic Effects/Carcinogenicity	Prolonged or repeated exposure may cause lung damage.
Other Information	None known.

Toxicity Tests

Oral Toxicity:	Not determined
Dermal Toxicity:	Not determined
Inhalation Toxicity:	Not determined
Primary Irritation Effect:	Not determined

Carcinogenicity	Not determined
Genotoxicity:	Not determined
Reproductive / Developmental Toxicity:	Not determined

12. ECOLOGICAL INFORMATION

Mobility (Water/Soil/Air)	Not determined
Persistence/Degradability	Not determined
Bio-accumulation	Not Determined

Ecotoxicological Information

Acute Fish Toxicity:	Not determined
Acute Crustaceans Toxicity:	Not determined
Acute Algae Toxicity:	Not determined
Chemical Fate Information	Not determined
Other Information	Not applicable

13. DISPOSAL CONSIDERATIONS

Disposal Method	Disposal should be made in accordance with federal, state, and local regulations.
Contaminated Packaging	Follow all applicable national or local regulations.

14. TRANSPORT INFORMATION

Land Transportation

DOT
Not restricted

Canadian TDG
Not restricted

ADR Not restricted

Air Transportation

ICAO/IATA
Not restricted

Sea Transportation

IMDG
Not restricted

Other Shipping Information

Labels:	None

15. REGULATORY INFORMATION

US Regulations

US TSCA Inventory	All components listed on inventory.
EPA SARA Title III Extremely Hazardous Substances	Not applicable
EPA SARA (311,312) Hazard Class	Acute Health Hazard
EPA SARA (313) Chemicals	This product contains toxic chemical(s) listed below which is(are) subject to the reporting requirements of Section 313 of Title III of SARA and 40 CFR Part 372: Aluminum//7429-90-5
EPA CERCLA/Superfund Reportable Spill Quantity For This Product	Not applicable.
EPA RCRA Hazardous Waste Classification	If product becomes a waste, it does NOT meet the criteria of a hazardous waste as defined by the US EPA.
California Proposition 65	All components listed do not apply to the California Proposition 65 Regulation.
MA Right-to-Know Law	One or more components listed.
NJ Right-to-Know Law	One or more components listed.
PA Right-to-Know Law	One or more components listed.

Canadian Regulations

Canadian DSL Inventory	All components listed on inventory.
WHMIS Hazard Class	B6 Reactive Flammable Materials D2B Toxic Materials

16. OTHER INFORMATION

The following sections have been revised since the last issue of this MSDS
Not applicable

Additional Information

For additional information on the use of this product, contact your local Halliburton representative.

For questions about the Material Safety Data Sheet for this or other Halliburton products, contact Product Stewardship at 1-580-251-4335.

Disclaimer Statement

This information is furnished without warranty, expressed or implied, as to accuracy or completeness. The information is obtained from various sources including the manufacturer and other third party sources. The information may not be valid under all conditions nor if this material is used in combination with other materials or in any process. Final determination of suitability of any material is the sole responsibility of the user.

END OF MSDS

HALLIBURTON

MATERIAL SAFETY DATA SHEET

Product Trade Name: **MICROBOND EXPANDING ADDITIVE**

Revision Date: 16-Feb-2004

1. CHEMICAL PRODUCT AND COMPANY IDENTIFICATION

Product Trade Name: MICROBOND EXPANDING ADDITIVE
Synonyms: None
Chemical Family: Mineral
Application: Additive

Manufacturer/Supplier
Halliburton Energy Services
P.O. Box 1431
Duncan, Oklahoma 73536-0431
Emergency Telephone: (800) 666-9260 or (713) 676-3000

Prepared By
Chemical Compliance
Telephone: 1-580-251-4335

2. COMPOSITION/INFORMATION ON INGREDIENTS

SUBSTANCE	CAS Number	PERCENT	ACGIH TLV-TWA	OSHA PEL-TWA
Sodium carbonate	497-19-8	1 - 5%	Not applicable	Not applicable
Calcium hydroxide	1305-62-0	10 - 30%	5 mg/m^3	5 mg/m^3
Calcium aluminate	12042-68-1	10 - 30%	2 mg/m^3	Not applicable
Calcium sulfate		60 - 100%	10 mg/m^3	15 mg/m^3

3. HAZARDS IDENTIFICATION

Hazard Overview May cause eye, skin, and respiratory irritation.

4. FIRST AID MEASURES

Inhalation If inhaled, remove from area to fresh air. Get medical attention if respiratory irritation develops or if breathing becomes difficult.

Skin Wash with soap and water. Get medical attention if irritation persists.

Eyes In case of contact, immediately flush eyes with plenty of water for at least 15 minutes and get medical attention if irritation persists.

Ingestion Do not induce vomiting. Slowly dilute with 1-2 glasses of water or milk and seek medical attention. Never give anything by mouth to an unconscious person.

Notes to Physician Not Applicable

5. FIRE FIGHTING MEASURES

Flash Point/Range (F):	Not Determined
Flash Point/Range (C):	Not Determined
Flash Point Method:	Not Determined
Autoignition Temperature (F):	Not Determined
Autoignition Temperature (C):	Not Determined
Flammability Limits in Air - Lower (%):	Not Determined
Flammability Limits in Air - Upper (%):	Not Determined

Fire Extinguishing Media All standard firefighting media.

Special Exposure Hazards Decomposition in fire may produce toxic gases.

Special Protective Equipment for Fire-Fighters Full protective clothing and approved self-contained breathing apparatus required for fire fighting personnel.

NFPA Ratings: Health 1, Flammability 0, Reactivity 0
HMIS Ratings: Flammability 0, Reactivity 0, Health 1

6. ACCIDENTAL RELEASE MEASURES

Personal Precautionary Measures Use appropriate protective equipment. Avoid creating and breathing dust.

Environmental Precautionary Measures Prevent from entering sewers, waterways, or low areas.

Procedure for Cleaning / Absorption Scoop up and remove.

7. HANDLING AND STORAGE

Handling Precautions Avoid contact with eyes, skin, or clothing. Avoid creating or inhaling dust.

Storage Information Store in a cool, dry location.

8. EXPOSURE CONTROLS/PERSONAL PROTECTION

Engineering Controls Use in a well ventilated area.

Respiratory Protection Dust/mist respirator. (95%)

Hand Protection Normal work gloves.

Skin Protection Normal work coveralls.

Eye Protection Wear safety glasses or goggles to protect against exposure.

Other Precautions None known.

9. PHYSICAL AND CHEMICAL PROPERTIES

Physical State:	Solid
Color:	Light red
Odor:	Odorless
pH:	Not Determined
Specific Gravity @ 20 C (Water=1):	3.2
Density @ 20 C (lbs./gallon):	Not Determined
Bulk Density @ 20 C (lbs/ft3):	59.4
Boiling Point/Range (F):	Not Determined

Boiling Point/Range (C):	Not Determined
Freezing Point/Range (F):	Not Determined
Freezing Point/Range (C):	Not Determined
Vapor Pressure @ 20 C (mmHg):	Not Determined
Vapor Density (Air=1):	Not Determined
Percent Volatiles:	Not Determined
Evaporation Rate (Butyl Acetate=1):	Not Determined
Solubility in Water (g/100ml):	Insoluble
Solubility in Solvents (g/100ml):	Not Determined
VOCs (lbs./gallon):	Not Determined
Viscosity, Dynamic @ 20 C (centipoise):	Not Determined
Viscosity, Kinematic @ 20 C (centistrokes):	Not Determined
Partition Coefficient/n-Octanol/Water:	Not Determined
Molecular Weight (g/mole):	>600

10. STABILITY AND REACTIVITY

Stability Data:	Stable
Hazardous Polymerization:	Will Not Occur
Conditions to Avoid	None anticipated
Incompatibility (Materials to Avoid)	None known.
Hazardous Decomposition Products	Oxides of sulfur. Carbon monoxide and carbon dioxide.
Additional Guidelines	Not Applicable

11. TOXICOLOGICAL INFORMATION

Principle Route of Exposure	Eye or skin contact, inhalation.
Inhalation	May cause respiratory irritation. May cause allergic respiratory reaction.
Skin Contact	May cause mild skin irritation.
Eye Contact	May cause mild eye irritation.
Ingestion	Irritation of the mouth, throat, and stomach.
Aggravated Medical Conditions	None known.
Chronic Effects/Carcinogenicity	No data available to indicate product or components present at greater than 1% are chronic health hazards.
Other Information	None known.

Toxicity Tests

Oral Toxicity:	Not determined
Dermal Toxicity:	Not determined
Inhalation Toxicity:	Not determined
Primary Irritation Effect:	Not determined
Carcinogenicity	Not determined
Genotoxicity:	Not determined

Reproductive / Developmental Toxicity:	Not determined

12. ECOLOGICAL INFORMATION

Mobility (Water/Soil/Air)	Not determined
Persistence/Degradability	Not determined
Bio-accumulation	Not Determined

Ecotoxicological Information

Acute Fish Toxicity:	Not determined
Acute Crustaceans Toxicity:	Not determined
Acute Algae Toxicity:	Not determined

Chemical Fate Information	Not determined
Other Information	Not applicable

13. DISPOSAL CONSIDERATIONS

Disposal Method	Bury in a licensed landfill according to federal, state, and local regulations.
Contaminated Packaging	Follow all applicable national or local regulations.

14. TRANSPORT INFORMATION

Land Transportation

DOT
Not restricted

Canadian TDG
Not restricted

ADR Not restricted

Air Transportation

ICAO/IATA
Not restricted

Sea Transportation

IMDG
Not restricted

Other Shipping Information

Labels:	None

15. REGULATORY INFORMATION

US Regulations

US TSCA Inventory	All components listed on inventory.
EPA SARA Title III Extremely Hazardous Substances	Not applicable
EPA SARA (311,312) Hazard Class	None
EPA SARA (313) Chemicals	This product does not contain a toxic chemical for routine annual "Toxic Chemical Release Reporting" under Section 313 (40 CFR 372).
EPA CERCLA/Superfund Reportable Spill Quantity For This Product	Not applicable.
EPA RCRA Hazardous Waste Classification	If product becomes a waste, it does NOT meet the criteria of a hazardous waste as defined by the US EPA.
California Proposition 65	All components listed do not apply to the California Proposition 65 Regulation.
MA Right-to-Know Law	One or more components listed.
NJ Right-to-Know Law	One or more components listed.
PA Right-to-Know Law	One or more components listed.

Canadian Regulations

Canadian DSL Inventory	Product contains one or more components not listed on inventory.
WHMIS Hazard Class	Un-Controlled

16. OTHER INFORMATION

The following sections have been revised since the last issue of this MSDS
Not applicable

Additional Information

For additional information on the use of this product, contact your local Halliburton representative.

For questions about the Material Safety Data Sheet for this or other Halliburton products, contact Chemical Compliance at 1-580-251-4335.

Disclaimer Statement

This information is furnished without warranty, expressed or implied, as to accuracy or completeness. The information is obtained from various sources including the manufacturer and other third party sources. The information may not be valid under all conditions nor if this material is used in combination with other materials or in any process. Final determination of suitability of any material is the sole responsibility of the user.

END OF MSDS